Strong decay widths and mass spectra of charmed baryons

H. García-Tecocoatzi

Center for High Energy Physics, Kyungpook National University, 80 Daehak-ro, Daegu 41566, Korea and INFN, Sezione di Genova, Via Dodecaneso 33, 16146 Genova, Italy

A. Giachino

INFN, Sezione di Genova, Via Dodecaneso 33, 16146 Genova, Italy and Institute of Nuclear Physics Polish Academy of Sciences, Radzikowskiego 152, 31-342 Cracow, Poland

J. Li and A. Ramirez-Morales

Center for High Energy Physics, Kyungpook National University, 80 Daehak-ro, Daegu 41566, Korea

E. Santopinto*

INFN, Sezione di Genova, Via Dodecaneso 33, 16146 Genova, Italy

(Received 8 July 2022; accepted 26 September 2022; published 27 February 2023)

The total decay widths of the charmed baryons are calculated by means of the $^3P_0$ model. Our calculations consider in the final states: the charmed baryon-(vector/pseudoscalar) meson pairs and the (octet/decuplet) baryon-(pseudoscalar/vector) charmed meson pairs, within a constituent quark model. Furthermore, we calculate the masses of the charmed baryon ground states and their excitations up to the D-wave in a constituent quark model both in the three-quark and in the quark-diquark schemes, utilizing a Hamiltonian model based on a harmonic oscillator potential plus a mass splitting term that encodes the spin, spin-orbit, isospin, and flavor interactions. The parameters of the Hamiltonian model are fitted to the experimental data of the charmed baryon masses and decay widths. As the experimental uncertainties of the data affect the fitted model parameters, we have thoroughly propagated these uncertainties into our predicted charmed baryon masses and decay widths via a Monte Carlo bootstrap approach, which is often absent in other theoretical studies on this subject. Our quantum number assignments and predictions of the masses and strong partial decay widths are in reasonable agreement with the available data. Thus, our results show the ability to guide future measurements in LHCb, Belle and Belle II experiments. Finally, the appendices provide some details of our calculations, in which we include the flavor coupling coefficients, which are useful for further theoretical investigations.

DOI: 10.1103/PhysRevD.107.034031

I. INTRODUCTION

The discovery of new baryon resonances in high-energy physics experiments always enriches our knowledge of the hadron zoo, and provides essential information to explain the fundamental forces that govern nature. In particular, the hadron mass patterns carry information regarding the way the quarks interact with one another, and provide further insight into the fundamental binding mechanism of matter at an elementary level.

*elena.santopinto@ge.infn.it

The number of observed charmed baryons has increased owing to the LHCb and Belle experiments. In 2017, the LHCb collaboration announced the observation of five narrow Ω_c states in the $\Xi_c^+ K^-$ decay channel [1]. Later, Belle observed five resonant states in the $\Xi_c^+ K^-$ invariant mass distribution and unambiguously confirmed four of the states announced by LHCb, $\Omega_c(3000)$, $\Omega_c(3050)$, $\Omega_c(3066)$, and $\Omega_c(3090)$, although no signal was found for the $\Omega_c(3119)$ state [2]. Belle also measured a signal excess at 3188 MeV, corresponding to the $\Omega_c(3188)$ state reported by LHCb [2]. In 2020, the LHCb collaboration observed three new states, $\Xi_c^0(2923)$, $\Xi_c^0(2939)$, and $\Xi_c^0(2965)$ [3]; however, their J^P quantum numbers were not reported. These results reported by LHCb implied that the $\Xi_c^0(2930)$ broad state observed by Belle [4] and *BABAR* [5] resolves into two narrower states $\Xi_c^0(2923)$ and

$\Xi_c^0(2939)$. Nevertheless, a puzzle emerges in the experimental data, since Ref. [3] reported a narrow state with a central mass of about 2965 MeV, which is close to a resonance seen by the Belle collaboration at 2970 MeV [6,7], and confirmed by the *BABAR* collaboration [8]; hence, further studies are required in order to determine whether these observations correspond to different baryons or to the same one. Moreover, the available charm baryon data are limited, especially for the Σ_c resonances; indeed, only three states are reported by the PDG [9], $\Sigma_c(2455)$, $\Sigma_c(2520)$ and $\Sigma_c(2800)$, while new analyses are being carried out in this sector [10]. More recently in 2021, the Belle collaboration measured the spin and parity of the $\Xi_c(2970)$ state to be $J^P = 1/2^+$ [11], under an assumption that the lowest partial wave dominates the decay.

The application of the nonrelativistic quark model to the light baryon spectrum owes its origins to the pioneering investigations by Isgur and Karl [12,13], which were further extended in [14] to the Λ_c and Σ_c baryons and to the Λ_b and Σ_b baryons in [15]. Over the last few years, the interest in heavy-light baryon spectroscopy has grown once more. Examples of the recent ample literature on theoretical investigations into the heavy baryon spectroscopy are: the reports of the QCD-motivated relativistic quark-diquark model based on the quasipotential approach [16,17], the nonrelativistic quark model [14,18–20], and the QCD sum rules in the framework of the Heavy Quark Effective Theory (HQET) [21–24], and the symmetry-preserving Schwinger-Dyson equation approach [25]. Alternative discussions employing other models can be found in Refs. [26–30], and lattice QCD studies in Refs. [31–34]. For extra references, see the review articles [35–39]. The spin-parity quantum numbers for most of the charmed baryon states which are reported by the PDG [9] are not measured yet, but they have been extracted from quark model predictions. Furthermore, it is unclear whether the heavy baryons behave as quark-diquark or three-quark systems. Thus, a full understanding of the internal structure of the charmed baryons still requires thorough theoretical and experimental studies.

Numerous studies have been conducted on the heavy baryon decay widths. Nevertheless, a complete calculation of all charmed baryon partial strong decay widths for ground and excited states up to the D-wave shell within the same model has never been performed. For example, within the framework of the chiral quark models in Ref. [40], only the open-flavor strong decay widths $\Lambda_c \to \Sigma_c\pi, D^0 p$ and $\Sigma_c \to \Lambda_c\pi, \Sigma_c\pi, D^0 p$ were calculated. Additionally, in Ref. [41] the Ξ_c' strong decays were considered up to the D-wave shell, while no predictions of the other charmed baryon decays were made. In Refs. [42,43] the authors calculated the S- and P-wave heavy baryon decay widths; however, their analysis was limited to baryons decaying only into ground-state charmed baryons plus pseudoscalar mesons. Moreover, no D-wave or radial excitations were reported. In the framework of the heavy hadron chiral perturbation theory in Ref. [44], certain decays of charmed baryons Λ_c, Σ_c, and Ξ_c' baryons were computed although these calculations did not include the charmed baryon-vector meson channels and did not give predictions for the Ω_c states. In Ref. [45] the calculations were performed only for the S- and P-wave Λ_c, Σ_c, and Ξ_c' states that decay into a ground-state charmed baryon plus a pion. Adopting a nonrelativistic quark model, in Ref. [46] only the decay widths of the charmed baryons $\Lambda_c^*(2595)$, $\Lambda_c^*(2625)$, $\Lambda_c^*(2765)$, $\Lambda_c^*(2880)$, and $\Lambda_c^*(2940)$ into $\Sigma_c(2455)\pi$ and $\Sigma_c^*(2520)\pi$, and of $\Sigma_c(2455)$ and $\Sigma_c^*(2520)$ into $\Lambda_c\pi$, were evaluated. In a more recent work [47], the same decay widths were calculated by adding relativistic corrections, and the previous analysis was extended to the decay widths of bottom baryons. In the context of the elementary emission model [48], the strong and radiative decays of charmed and bottom baryons were investigated. However, the study was restricted to the low-lying λ-mode D-wave excitations and the charmed baryon-vector meson channels or the charmed meson-octet/decuplet baryon channels were not included. In the framework of QCD sum rules in Ref. [49], the author studied only the P-wave $\Lambda_c \to \Sigma_c + \pi$ decays and the P-wave Λ_c electromagnetic decays, while in [50] the authors calculated the P-wave charmed baryon decays into ground-state charmed baryons accompanied by a pseudoscalar meson. In [51], the $^3P_0$ model was applied to calculate the strong decays of Λ_c, Σ_c, and Ξ_c excited states up to the D-wave shell. Nevertheless the decay widths into charmed baryon-vector mesons were not calculated, nor was the Ω_c sector considered. The $^3P_0$ model was also applied in [52–54]. In these references, however only the Λ_c decays were studied. In [20], the Eichten, Hill and Quigg formula, in combination with the $^3P_0$ model, was applied in order to calculate the $1P$ and $2S$ Λ_c, Σ_c and Ξ_c decays into charmed baryon and pseudoscalar mesons.

In Ref. [55], prompted by the observation of the five Ω_c by LHCb [1], we calculated the Ω_c decay widths in the $\Xi_c^+ K^-$ and $\Xi_c'^+ K^-$ channels within the $^3P_0$ model. In that study, we also calculated the Ω_b decay widths in the $\Xi_b^+ K^-$ and $\Xi_b'^+ K^-$ channels and gave predictions for the mass spectra of both Ω_c and Ω_b ground states and P-wave excitations. Subsequently, in Ref. [56], we extended our model to the Ξ_c' and the Ξ_b' states and calculated the mass spectra and the strong partial decay widths of the Ξ_c'-ground states and P-wave excitations into $^2\Sigma_c\bar{K}$, $^2\Xi_c'\pi$, $^4\Sigma_c\bar{K}$, $^4\Xi_c'\pi$, $\Lambda_c\bar{K}$, $\Xi_c\pi$, and $\Xi_c\eta$ and of the Ξ_b'-ground states and P-wave excitations into $^2\Sigma_b\bar{K}$, $^2\Xi_b'\pi$, $^4\Sigma_b\bar{K}$, $^4\Xi_b'\pi$, $\Lambda_b\bar{K}$, $\Xi_b\pi$, and $\Xi_b\eta$, within both the elementary emission model (EEM) and the $^3P_0$ model. In the present article we further extend our model to the whole charmed baryon states (cqq, cqs and css systems) by employing the same mass formula originally introduced in Ref. [55]. Additionally, in the present paper, the parameters of the model are fitted in order to globally reproduce all the available charmed baryon experimental states. The experimental uncertainties are also propagated to the model parameters by means of the Monte Carlo bootstrap method [57], which is an advanced method used to properly estimate the error propagation by taking into account the correlation between the fitted parameters. In this way, we perform a global fit of a single model, in which the same set of parameters predicts the charmed baryon masses and strong partial decay. Moreover, considering the well-established observation by Isgur and Karl in Ref. [12] that the harmonic oscillator wave functions are a good approximation of the eigenfunctions of low-lying states, and also taking into account that the calculations of the strong decay widths are barely sensitive to the specific model used [58], our strong partial decay width predictions are the most complete calculations in the charmed baryon sector up to date. The paper is organized as follows: in Sec. II, we introduce the details of the methodology used to construct the charmed baryon states and to calculate the mass spectra and decay widths. The theoretical details for the calculation of the charmed baryon mass spectra include contributions due to spin-orbit-, spin-, isospin- and flavor-dependent interactions. Thus, we develop a formalism for obtaining the S-, P-, and D-wave charmed baryon mass spectrum. We also describe the calculation of the total decay widths of the charmed baryons via the ${}^3P_0$. In Sec. III, we carefully study the parameters of the mass formula presented in Ref. [55] and perform a global fit to the data on the well-established charmed baryons and their uncertainties, which have been propagated by means of the bootstrap method. In Sec. IV, we present the masses and widths of all charmed baryons up to D-wave and discuss our assignments for all the available experimental data. In Sec. V, we discuss why the presence or absence of the ρ-mode excitations in the experimental spectrum is the key to distinguishing between the quark-diquark and three-quark behaviors [55]. Finally, in Sec. VI, we state our conclusions.

II. METHODOLOGY

A. Mass spectra of charmed baryons

The masses of the charmed baryon states are calculated as the eigenvalues of the Hamiltonian of Ref. [55], which is modeled as:

$$H = H_{\text{h.o.}} + P_s \mathbf{S}^2 + P_{sl} \mathbf{S}\cdot\mathbf{L} + P_I \boldsymbol{I}^2 + P_f \mathbf{C_2}(\text{SU}(3)_\text{f}), \quad (1)$$

$\mathbf{S}$, $\mathbf{L}$, $\boldsymbol{I}$ and $\mathbf{C_2}(\text{SU}(3)_\text{f})$ are the spin, orbital momentum, isospin and Casimir operators, respectively. These terms are weighted with the model parameters P_s, P_{sl}, P_I and P_f, as indicated in Eq. (1). Notice that our mass formula in Eq. (1) is independent of I_z, the isospin projection; therefore, the charge channels are degenerated in this model.

For the case in which the baryon is modeled as a three-quark system, the three-dimensional h.o. Hamiltonian reads as,

$$H_{\text{h.o.}} = \sum_{i=1}^{3} m_i + \frac{\mathbf{p}_\rho^2}{2m_\rho} + \frac{\mathbf{p}_\lambda^2}{2m_\lambda} + \frac{1}{2} m_\rho \omega_\rho^2 \boldsymbol{\rho}^2 + \frac{1}{2} m_\lambda \omega_\lambda^2 \boldsymbol{\lambda}^2 \quad (2)$$

written in terms of Jacobi coordinates, $\boldsymbol{\rho}$ and $\boldsymbol{\lambda}$, and conjugated momenta, $\mathbf{p}_\rho$ and $\mathbf{p}_\lambda$. The $H_{\text{h.o}}$ eigenvalues are

$$\sum_{i=1}^{3} m_i + \omega_\rho n_\rho + \omega_\lambda n_\lambda; \quad \text{with} \quad \omega_{\rho(\lambda)} = \sqrt{\frac{3K_c}{m_{\rho(\lambda)}}}, \quad (3)$$

where m_i are the constituent quark masses, m_1 and m_2 correspond to the light quarks and m_3 to the charm quark; m_ρ is defined as $m_\rho = (m_1 + m_2)/2$, and $m_\lambda = 3m_\rho m_3/(2m_\rho + m_3)$. We use the well-known definitions for $n_{\rho(\lambda)} = 2k_{\rho(\lambda)} + l_{\rho(\lambda)}$, $k_{\rho(\lambda)} = 0, 1, \ldots,$ and $l_{\rho(\lambda)} = 0, 1, \ldots$; here, $l_{\rho(\lambda)}$ are the orbital angular momenta of the $\rho(\lambda)$ oscillators, and $k_{\rho(\lambda)}$ is the number of nodes (radial excitations) in the $\rho(\lambda)$ oscillators. K_c is the spring constant.

Additionally, we present a simplification of the three-quark system that utilizes only one relative coordinate $\mathbf{r}$ and momentum $\mathbf{p}_r$, namely, the quark-diquark system. Here, the two light quarks are regarded as a single diquark object. The quark-diquark Hamiltonian reads as,

$$H_{\text{h.o.}} = m_D + m_c + \frac{\mathbf{p}_r^2}{2\mu} + \frac{1}{2}\mu\omega_r^2 \mathbf{r}^2, \quad (4)$$

with $\mathbf{p}_r = (m_c \mathbf{p}_D - m_D \mathbf{p}_c)/(m_c + m_D)$. The $H_{\text{h.o}}$ eigenvalues are

$$m_D + m_c + \omega_r n_r; \quad \text{with} \quad \omega_r = \sqrt{\frac{3K_c}{\mu}}, \quad (5)$$

where m_D is the diquark mass, m_c is the charm quark mass; μ is the reduced mass of the system, and is defined as $\mu = m_c m_D/(m_c + m_D)$; n_r and K_c are defined as in the three-quark system.

B. Charmed baryon states

In the three-quark model, the baryon states are thought as a qqQ system, where $Q = c$ and $q = u$, d, s. The three-quark Hamiltonian in Eq. (2) is expressed in terms of two coordinates, $\boldsymbol{\rho}$ and $\boldsymbol{\lambda}$ [59], that encode the spatial degrees of freedom of the system with associated effective masses, m_ρ and m_λ. Note that in heavy-light baryons, for which $m_\rho \ll m_\lambda$, the two excitation modes can be decoupled from each other as long as the heavy-light quark mass difference is significant.

In the quark-diquark system, the baryon states are thought as a DQ system, where $Q = c$ and $D = D_\Omega, D_\Xi, D_{\Sigma,\Lambda}$ are the diquarks that correspond to the Ω_c, $\Xi'_c(\Xi_c)$, Σ_c and Λ_c baryons, respectively. The quark-diquark Hamiltonian in Eq. (4) is expressed in terms of one spatial coordinate $\mathbf{r}$ with an associated reduced mass μ; i.e., the quark-diquark system resembles a diatomic molecule.

We construct the ground and excited states in order to establish the quantum numbers of the charmed baryon states. We consider that a single quark is described by its spin, flavor, color, and spatial degrees of freedom. The baryon states should be in color singlet. Moreover, in our models, the light quarks are considered to be identical particles; hence, their wave function should be antisymmetric in order to satisfy the Pauli Principle. Since the two light quarks should be in the $\bar{\mathbf{3}}_c$, their spin-flavor and orbital wave functions should have the same permutation symmetry: spin-flavor symmetric in the S-wave or D-wave ($\bar{\mathbf{3}}_f$ with spin 0 or $\mathbf{6}_f$ with spin 1), and spin-flavor anti-symmetric in the P-wave ($\bar{\mathbf{3}}_f$ with spin 1 or $\mathbf{6}_f$ with spin 0).

Formally, a three-quark (quark-diquark) quantum state, written as $|l_\lambda(l_r), l_\rho, k_\lambda(k_r), k_\rho\rangle$, is defined by its total angular momentum $\mathbf{J}_{tot} = \mathbf{L}_{tot} + \mathbf{S}_{tot}$, where $\mathbf{L}_{tot} = \mathbf{l}_\rho + \mathbf{l}_\lambda$ ($\mathbf{L}_{tot} = \mathbf{l}_r$) and $\mathbf{S}_{tot} = \mathbf{S}_{lt} + \frac{1}{2}$, $\mathbf{S}_{lt}$ is the coupled spin of the light quarks and the number of nodes is $k_{\lambda,\rho}(k_r)$. In addition, in order to unambiguously define these quantum states, we assign to them the flavor $\mathcal{F}$ and spectroscopy $^{2S+1}L_J$ representations. In the following paragraphs, we will construct the possible states for the two different flavor representations available for the charmed baryons, in the energy bands $N = n_\rho + n_\lambda$ ($N = n_r$) and $N = 0$, 1, 2 in order to find S-, P-, D-wave charmed baryon states.

1. The symmetric $\mathbf{6}_f$*-multiplet for the three-quark model*

The Ω_c, Ξ'_c, and Σ_c baryons form a flavor sextet in the charmed baryon sector. These charmed baryons have a symmetric flavor-wave function of the light quarks which, in combination with their antisymmetric color-wave function, produces an antisymmetric wave function. This implies that the product of the spatial and spin-wave functions of the light quarks should be symmetric. In the energy band $N = 0$, if $l_\rho = l_\lambda = 0$, the spatial wave function of the two light quarks is symmetric. That is, these states have a symmetric-spin wave function of the two light quarks, meaning $\mathbf{S}_{lt} = \mathbf{1}$. Hence, two ground states, $\mathbf{J}_{tot} = \mathbf{S}_{tot} = \mathbf{1/2}, \mathbf{3/2}$, exist. For the energy band $N = 1$, there are two different possibilities. If $l_\rho = 0$ and $l_\lambda = 1$, we again have spatial-symmetric wave functions under the interchange of light quarks, which must be coupled with two possible spin configurations, $\mathbf{S}_{tot} = \mathbf{1/2}, \mathbf{3/2}$, with $\mathbf{L}_{tot} = \mathbf{1}$, yielding five P_λ-wave excitations. If $l_\rho = 1$ and $l_\lambda = 0$, the spatial wave function is antisymmetric under the interchange of light quarks implying that the two light quarks spin wave function is antisymmetric, meaning $\mathbf{S}_{lt} = \mathbf{0}$, which yields two P_ρ-wave states obtained from $\mathbf{J}_{tot} = \mathbf{1} + \mathbf{1/2} = \mathbf{1/2}, \mathbf{3/2}$. In the energy band $N = 2$, when $l_\rho = 0$ and $l_\lambda = 2$, the total spatial wave function is symmetric. Thus, it must be combined with two possible spin configurations, $\mathbf{S}_{tot} = \mathbf{1/2}, \mathbf{3/2}$, obtaining six D_λ-wave excitations. Additionally, there are radial excitation modes in this band. For the case $k_\rho = 0$ and $k_\lambda = 1$, the spatial wave function is symmetric. Thus, the two light quark spin wave function must also be symmetric, yielding two λ-radial excitations, $\mathbf{J}_{tot} = \mathbf{S}_{tot} = \mathbf{1/2}, \mathbf{3/2}$, since $\mathbf{L}_{tot} = \mathbf{0}$. The same situation appears when $k_\rho = 1$ and $k_\lambda = 0$; the spatial wave function is symmetric. Thus, there are two ρ-radial excitations, corresponding to $\mathbf{J}_{tot} = \mathbf{S}_{tot} = \mathbf{1/2}, \mathbf{3/2}$. In the case $l_\rho = 1$ and $l_\lambda = 1$, which yields $\mathbf{L}_{tot} = \mathbf{2}, \mathbf{1}, \mathbf{0}$, the two light quark spatial wave function is antisymmetric, implying that we have to couple it with the light quark antisymmetric spin configurations, $\mathbf{S}_{lt} = 0$, thus obtaining five possible states: two D-wave states, two P-wave states, and one S- wave state. Finally, if $l_\rho = 2$ and $l_\lambda = 0$, the spatial wave functions are symmetric. Hence, we have to combine them with $\mathbf{S}_{tot} = \mathbf{1/2}, \mathbf{3/2}$, obtaining six D_ρ-wave excitations.

2. The symmetric $\mathbf{6}_f$*-multiplet for the quark-diquark model*

When the Ω_c, Ξ'_c, and Σ_c baryons are seen as quark-diquark systems, the two constituent light quarks of the diquark are considered to be correlated, with no internal spatial excitations (S-wave); i.e., it is hypothesized that we are within the limit where the diquark internal spatial excitations are higher in energy than the scale of the resonances studied. Since the hadron must be colorless, the diquark transforms as $\bar{\mathbf{3}}$ under $SU_c(3)$; thus, the product of the spin and flavor wave functions of the diquark configuration should be symmetric. The flavor wave functions of the $\mathbf{6}_f$ representation are symmetric. As a result, we can only combine with axial-vector diquarks; that is, with $\mathbf{S}_{lt} = \mathbf{1}$. For the energy band $N = 0$, $\mathbf{L}_{tot} = \mathbf{0}$, and thus $\mathbf{J}_{tot} = \mathbf{S}_{tot} = \mathbf{1/2}, \mathbf{3/2}$, yielding two ground states. In the next band $N = 1$, $\mathbf{L}_{tot} = \mathbf{1}$ has to be coupled with $\mathbf{S}_{tot} = \mathbf{1/2}, \mathbf{3/2}$, yielding five P-wave excitations. For the band $N = 2$, $\mathbf{L}_{tot} = \mathbf{2}$, and we must combine with $\mathbf{S}_{tot} = \mathbf{1/2}, \mathbf{3/2}$, to get six D-wave states. Moreover, there is a radial degree of freedom $k = 1$; with $\mathbf{L}_{tot} = \mathbf{0}$, we have $\mathbf{J}_{tot} = \mathbf{S}_{tot} = \mathbf{1/2}, \mathbf{3/2}$, and hence find two radial excitations.

3. The antisymmetric $\bar{\mathbf{3}}_f$*-plet for the three-quark model*

The Λ_c and Ξ_c baryons form a flavor-antitriplet in the charmed baryon sector. These charmed baryons have an antisymmetric flavor wave function of the light quarks, and which, in combination with the antisymmetric color wave function, produces a symmetric combination. This implies that the product of the spatial and spin wave functions of the light quarks should be antisymmetric. For the energy band $N = 0$, if $l_\rho = l_\lambda = 0$, the spatial wave function of the two light quarks is symmetric, thus their spin wave function should be antisymmetric. This corresponds to $\mathbf{S}_{\rm lt} = \mathbf{0}$, producing only one ground state. For the energy band $N = 1$, if $l_\rho = 0$ and $l_\lambda = 1$, we have a light quark symmetric spatial wave function; thus, their spin wave function is antisymmetric. It implies $\mathbf{S}_{\rm tot} = \mathbf{1/2}$ and, in combination with the total $\mathbf{L}_{\rm tot} = \mathbf{1}$, yields two P_λ states. If $l_\rho = 1$ and $l_\lambda = 0$, the spatial wave function of the two light quarks is antisymmetric. Thus, their spin wave function is symmetric, giving two possible configurations: $\mathbf{S}_{\rm tot} = \mathbf{1/2}, \mathbf{3/2}$. This, in combination with $\mathbf{L}_{\rm tot} = \mathbf{1}$, constructs five P_ρ states. In the energy band $N = 2$, in the case of $l_\rho = 0$ and $l_\lambda = 2$, the total spatial wave function is symmetric; it is therefore combined with the light quark antisymmetric spin configuration, $\mathbf{S}_{\rm lt} = 0$, giving two D_λ-wave excitations. The two possible radial excitations, $k_\rho = 0$ and $k_\lambda = 1$, and $k_\rho = 1$ and $k_\lambda = 0$, are symmetric in the spatial wave function. They should be combined with the light quark antisymmetric spin configuration, $\mathbf{S}_{\rm lt} = 0$, producing one λ-radial excitation and one ρ-radial excitation. The antisymmetric spatial wave functions of the configuration $l_\rho = 1$ and $l_\lambda = 1$ are coupled to $\mathbf{L}_{\rm tot} = \mathbf{0}, \mathbf{1}, \mathbf{2}$, and the angular momenta should be combined with the symmetric spin configurations $\mathbf{S}_{\rm tot} = \mathbf{1/2}, \mathbf{3/2}$, coming from the light quark spin configuration, $\mathbf{S}_{\rm lt} = 1$, producing thirteen mixed excited states: six D-wave states, five P-wave states, and two S- wave states. Finally, the symmetric configuration $l_\rho = 2$ and $l_\lambda = 0$, combined with the light quark antisymmetric spin configuration, $\mathbf{S}_{\rm lt} = 0$, gives two D_ρ-wave excitations.

4. *The antisymmetric* $\bar{\mathbf{3}}_{\rm f}$*-plet for the quark-diquark model*

Moreover, Λ_c and Ξ_c baryons are described as quark-diquark systems. In this case, as discussed in Sec. II B 2, the diquark presents an S-wave configuration, given its lack of internal spatial excitations. Considering that it is $\bar{\mathbf{3}}$ in the color representation $SU_c(3)$, we conclude that the product of the spin and flavor wave functions of the diquark configuration should be symmetric. In the antisymmetric $\bar{\mathbf{3}}_{\rm f}$-plet, the flavor wave function is antisymmetric; thus, the spin wave function of the diquark correspond to a scalar configuration, $\mathbf{S}_{\rm lt} = \mathbf{0}$. For the energy band $N = 0$, we have $\mathbf{L} = \mathbf{0}$; thus, we only have one ground state $\mathbf{J}_{\rm tot} = \mathbf{S}_{\rm tot} = \mathbf{1/2}$. In the next band, $N = 1$, we must combine $\mathbf{L}$tot $= \mathbf{1}$ with $\mathbf{S}_{\rm tot} = \mathbf{1/2}$, which yields two P-wave states. In the band $N = 2$, we have $\mathbf{L}_{\rm tot} = \mathbf{1}$, and, on coupling to $\mathbf{S}_{\rm tot} = \mathbf{1/2}$, we get two D-wave states. Finally, with a radial excitation $k_r = 1$ and $\mathbf{L}_{\rm tot} = \mathbf{0}$, there is only one state.

C. Charmed baryon decay widths

The open-flavor strong decays of a charmed baryon A to another baryon B plus a meson C, $A \to BC$, have been studied by means of the $^3P_0$ model [51,60–62]. According to this model, a $q\bar{q}$ pair is created from the vacuum when a qqc baryon decays and regroups into an outgoing meson and a baryon via the quark rearrangement process as depicted in Fig. 1. In the present study, we consider the decay of a charmed baryon A to a charmed baryon B plus a light meson C, see Fig. 1(a), and also the case in which the final state is a light baryon B plus a charmed meson C, see Fig. 1(b). Within the nonrelativistic limit, the transition operator is written as

$$T^\dagger = -3\gamma_0 \sum_m \langle 1m; 1-m|00\rangle \int \mathrm{d}^3\mathbf{P}_4 \mathrm{d}^3\mathbf{P}_5 \delta^3(\mathbf{P}_4 + \mathbf{P}_5) \times \mathcal{Y}_1^m(\mathbf{P}_4 - \mathbf{P}_5)\chi_{1,-m}^{45}\varphi_0^{45}\omega_0^{45} b_4^\dagger(\mathbf{P}_4) d_5^\dagger(\mathbf{P}_5), \quad (6)$$

where 4 and 5 are the indices of the quark and antiquark created. $\varphi_0^{45} = (u\bar{u} + d\bar{d} + s\bar{s})/\sqrt{3}$ and $\omega_0^{45} = (r\bar{r} + b\bar{b} + g\bar{g})/\sqrt{3}$ are the flavor and color singlet-wave functions, respectively. $\chi_{1,-m}^{45}$ is the spin-triplet state. $\mathcal{Y}_1^m(\mathbf{k}) \equiv |\mathbf{k}| Y_1^m(\theta_k, \phi_k)$ is a solid harmonic polynomial corresponding to the P-wave quark pair. γ_0 is a dimensionless constant related to the strength of the $q\bar{q}$ pair creation vertex from the vacuum. γ_0 is a free parameter of the $^3P_0$ model.

The total decay width Γ is the sum of the partial widths for the open channels BC, $\Gamma = \sum_{BC} \Gamma_{A\to BC}$, where the partial widths $\Gamma_{A\to BC}$, are computed as

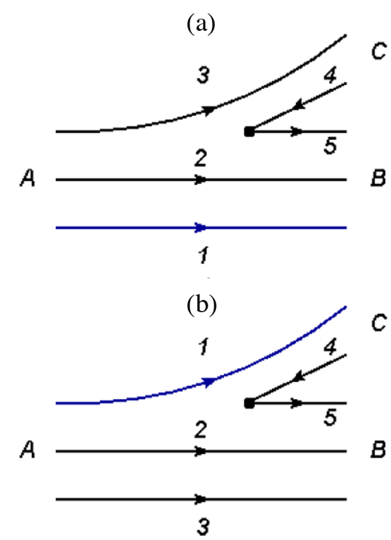

FIG. 1. The $^3P_0$ pair-creation model (color online). The blue line 1 denotes a charm quark, while the remaining black lines denote light quarks. In diagram (a) the charmed baryon A decays to a charmed baryon B and a light meson C. In diagram (b) the charmed baryon A decays to a light baryon and a charmed meson C.

$$\Gamma_{A\to BC} = \frac{2\pi\gamma_0^2}{2J_A+1}\Phi_{A\to BC}(q_0)\sum_{M_{J_A},M_{J_B}}|\mathcal{M}^{M_{J_A},M_{J_B}}|^2. \quad (7)$$

Here, $\mathcal{M} = \langle BC|T^\dagger|A\rangle$ is the $^3P_0$ amplitude written in terms of hadron h.o. wave functions and the sum runs over the projections M_{J_A,J_B} of the total angular momenta $J_{A,B}$ of A and B. q_0 is the relative momentum between B and C, and the coefficient $\Phi_{A\to BC}(q_0)$ is the relativistic phase space factor [62],

$$\Phi_{A\to BC}(q_0) = q_0\frac{E_B(q_0)E_C(q_0)}{m_A},$$
$$\text{with}\quad E_{B,C} = \sqrt{m_{B,C}^2+q_0^2};$$

where m_A is the initial charmed baryon mass in its rest frame. The masses m_B and m_C and energies E_B and E_C correspond to the final baryon and meson, respectively.

The h.o. wave functions depend on the parameters $\alpha_{\rho(\lambda)}$, see Appendix A, which, in Ref. [62], are regarded as free parameters. Conversely, in the present study, $\alpha_{\rho(\lambda)}$ are related to the baryon ρ- and λ-mode h.o. frequencies as defined in Eq. (3); this relation is established by $\alpha_{\rho(\lambda)}^2 = \omega_{\rho(\lambda)}m_{\rho(\lambda)}$. Therefore, $\alpha_{\rho(\lambda)}$ will depend on the fit parameter K_c and constituent quark masses. The h.o. wave functions and coordinate system conventions used in our decay width calculations are given in Appendix A. The decay widths are calculated for each charmed baryon type; the available open-flavor channels include all the pseudoscalar and vector mesons. The open-flavor channels share an extra parameter R related to the meson size, which has been discussed extensively in the literature [63–65]; we adopt $R = 2.1/\text{GeV}$ which is taken from Refs. [51,66]. The flavor-meson-wave functions are given in Appendix D. All the possible flavor couplings, $\mathcal{F}_{A\to BC} = \langle\phi_B\phi_C|\phi_0\phi_A\rangle$ are given in Appendix E. The masses of the decay products are listed in Table XIV in Appendix G. It is important to mention that the application of the $^3P_0$ model is restricted to the three-quark system, owing the difficulty of dealing with diquark spatial wave functions within the $^3P_0$ model formalism.

III. PARAMETER DETERMINATION AND UNCERTAINTIES

A. Mass spectra of charmed baryons

We fitted a selection of experimentally observed charmed baryon states, Ω_c, Σ_c, Λ_c, Ξ_c', and Ξ_c, to the masses predicted by Eq. (2) and Eq. (4) to obtain the constituent quark and diquark masses (m_c, m_s, $m_{u,d}$, m_{D_Ω}, m_{D_Ξ}, and $m_{D_{\Sigma,\Lambda}}$) and the model parameters (P_s, P_{sl}, P_I, P_f, and K_c). The fitted model parameters and masses minimize the sum of the squared differences between the experimental baryon masses and those predicted by the model (least-squares method).

The measured baryon masses come with statistical and systematic uncertainties. Furthermore, the models in Eq. (2) and Eq. (4) are approximate descriptions of the charm baryons. Thus, to take into account the possible deviations of these models from the experimental observations, we assigned a model uncertainty to each model. The model uncertainty, σ_{mod}, is calculated in accordance with Ref. [9] and is such that $\chi^2/\text{NDF} \simeq 1$, where

$$\chi^2 = \sum_i \frac{(M_{\text{mod},i} - M_{\text{exp},i})^2}{\sigma_{\text{mod}}^2 + \sigma_{\text{exp},i}^2}, \quad (8)$$

$M_{\text{mod},i}$ are the predicted charm baryon masses, $M_{\text{exp},i}$ are the experimental charm baryon masses included in the fit with uncertainties $\sigma_{\text{exp},i}$, and NDF is the number of degrees of freedom. We obtained $\sigma_{\text{mod}} = 15.42$ MeV for the three-quark model and $\sigma_{\text{mod}} = 13.63$ MeV for the quark-diquark model.

To integrate the experimental and model uncertainties into our fit, we carried out a statistical simulation of error propagation. To do so, we randomly sampled the experimental masses from a Gaussian shaped distribution with a mean equal to the central mass value and a width equal to the squared sum of the uncertainties. We fitted the model by using a sampled mass corresponding to each experimental observed state included in the fit, and we repeated the procedure 10^4 times. In this manner, we obtained a Gaussian distribution for each constituent quark mass, model parameter, and the baryon mass itself. Next, we assigned the mean of the distribution as the value of the parameter and used its difference from the distribution quantiles at 68% confidence level (CL), in order to extract the uncertainty. This method is known as the Monte Carlo bootstrap uncertainty propagation [57,67].

The experimental masses and their corresponding uncertainties used in the fit and error propagation are marked with (*) in Tables IV–VII. These mass measurements are summarized in the PDG database [9]. However, the charmed baryon masses predicted by Eq. (2) are degenerated in comparison with different u or d quark configurations, since the model will assign identical masses to baryons with the same number of u or d quark contents. This is a consequence of isospin symmetry. As these groups of mass states have the same quantum numbers, our quantum number assignments are not affected by the mass degeneracy. In our calculations, to account for this degeneracy, we fitted the arithmetic mean of the measured masses and adopted a conservative approach to the uncertainty by defining it as the standard deviation among the measured masses, plus their highest reported experimental uncertainty. The calculations were carried out by using MINUIT [68] and NUMPY [69]. The results of the fit are shown in Table I. The constituent quark masses obtained agree with

TABLE I. Fitted parameters for the three-quark model (second column) and the quark-diquark model (third column). The † indicates that the parameter is absent in that model.

Parameter	Three-quark value	Diquark value
m_c	1606^{+58}_{-61} MeV	1563^{+22}_{-24} MeV
m_s	455^{+29}_{-27} MeV	†
$m_{u,d}$	284^{+30}_{-31} MeV	†
m_{D_Ω}	†	947^{+3}_{-3} MeV
m_{D_Ξ}	†	791^{+18}_{-14} MeV
$m_{D_{\Sigma,\Lambda}}$	†	613^{+20}_{-17} MeV
K_c	$0.0290^{+0.0007}_{-0.0008}$ GeV^3	$0.0195^{+0.0007}_{-0.0007}$ GeV^3
P_s	23^{+3}_{-3} MeV	24^{+3}_{-3} MeV
P_{sl}	18^{+5}_{-5} MeV	17^{+5}_{-5} MeV
P_I	45^{+8}_{-8} MeV	41^{+9}_{-9} MeV
P_f	52^{+6}_{-6} MeV	52^{+7}_{-7} MeV

TABLE II. Correlation between fitted parameters: three-quark system.

	m_c	m_s	m_n	K_c	P_s	P_{sl}	P_I	P_f
m_c	1							
m_s	−0.76	1						
$m_{u,d}$	−0.82	0.76	1					
K_c	−0.77	0.7	0.69	1				
P_s	0.26	−0.29	−0.27	−0.14	1			
P_{sl}	−0.1	0.08	0.08	0.37	−0.21	1		
P_I	0.11	0.12	−0.19	−0.16	0.21	−0.02	1	
P_f	−0.42	0.04	0.28	0.36	−0.51	0.21	−0.68	1

TABLE III. Correlation between fitted parameters: quark-diquark system.

	m_c	m_{D_Ω}	m_{D_Ξ}	$m_{D_{\Sigma,\Lambda}}$	K_c	P_s	P_{sl}	P_I	P_f
m_c	1								
m_{D_Ω}	0.0	1							
m_{D_Ξ}	0.0	0.85	1						
$m_{D_{\Sigma,\Lambda}}$	0.0	−0.83	0.3	1					
K_c	0.0	0.33	0.3	−0.52	1				
P_s	0.0	−0.18	−0.1	0.18	−0.14	1			
P_{sl}	0.0	0.14	0.1	−0.18	0.37	−0.21	1		
P_I	0.0	−0.72	−0.78	0.63	−0.16	0.21	−0.02	1	
P_f	0.0	0.7	0.68	−0.88	0.36	−0.51	0.21	−0.68	1

previous theoretical determinations [13]. Furthermore, the model parameters used in the present study are in the range of our previous work [55], where phenomenological considerations were considered to determine them. Tables II and III show the correlation of the fitted parameters in the three-quark and quark-diquark model, respectively. In the three-quark model, the constituent quark masses are highly correlated, indicating that the quark masses exhibit similar behavior inside the baryon. Moreover, the spring constant K_c is also highly correlated with the quark masses, as expected from Eq. (3). In the quark-diquark model, the charmed quark mass is totally uncorrelated with the diquark masses; this is a consequence of the diatomic structure of the modeled baryon. In the same manner, K_c is correlated with the diquark masses, as expected from Eq. (5).

B. Charmed baryon decay widths

The parameter determination and the error propagation for the decay widths were carried out in analogy with the above procedure for the charmed baryon masses. The pair-creation constant γ_0 of Eq. (7) was obtained by fitting data of selected charmed baryon decay widths.

To compute the uncertainty of the decay widths, we considered all possible sources of uncertainty. First, the error coming from the baryon mass m_A and parameter K_c were included by calculating a decay width for all the statistically simulated constituent quark masses, m_A and K_c and γ_0; each width calculation was then repeated 10^4 times. Next, we included the experimental uncertainties of the decay products m_B and m_C. These experimental uncertainties, the values of which are shown in Table XIV, were propagated to the decay widths by means of the same random sampling technique described for the masses. Furthermore, a model uncertainty, $\sigma_{\rm mod} = 4.44$, was included. We set the decay width value as the population mean of the Gaussian distribution obtained, with an error equivalent to the difference between this mean and the distribution quantiles at 68% CL. The value and uncertainty obtained are $\gamma_0 = 19.6 \pm 5.1$. These calculations are only performed when the charmed baryons are modeled as three-quark systems.

IV. RESULTS AND DISCUSSION

In this section, we present our results regarding the mass spectra and total decay widths of charmed baryons. The mass spectra are computed via the mass formula of Eq. (1). The theoretical masses and their uncertainties are reported in the third column for the three-quark system and in the fourth column for the quark-diquark system in Tables IV–VIII. The theoretical decay widths for the three-quark system are computed by using the $^3P_0$ model described in Sec. II C. The masses used in the decay width calculations are the three-quark model theoretical predictions of Tables IV–VIII. Each open-flavor channel decay width is obtained via Eq. (7), and the total decay width is the sum over all the channels. The theoretical total-decay widths and their uncertainties for the three-quark system are reported in the fifth column of Tables IV–VIII. The partial decay widths in the open-flavor channels are reported in Tables IX–XIII of Appendix F. In Tables IX–XIII, the partial decay widths denoted by 0 are forbidden by phase space, while the ones denoted by—are forbidden by selection rules.

Our proposed quantum number assignments for the charmed baryon states are summarized in Figs. 2–6 within the three-quark model. There is a good agreement between the predicted mass pattern spectrum and the experimental data. Furthermore, we present our charmed baryon spectrum on using the quark-diquark framework in Figs. 7–11. In the following subsections, we discuss our assignments to the available data reported in the PDG [9].

TABLE IV. $\Omega_c(ssc)$ states. The flavor multiplet is specified with the symbol $\mathcal{F}$. The first column shows the quantum states $|l_\lambda(l_r), l_\rho, k_\lambda(k_r), k_\rho\rangle$ for the three-quark (quark-diquark) model, where $l_{\lambda,\rho}(l_r)$ are the orbital angular momenta and $k_{\lambda,\rho}(k_r)$ the number of nodes of the $\lambda(r)$ and ρ oscillators. Furthermore, $N = n_\rho + n_\lambda$ $(N = n_r)$ separate the energy bands $N = 0, 1, 2$. The second column contains the spectroscopic notation $^{2S+1}L_J$ for each state and is defined by the total angular momentum $\mathbf{J}_{\rm tot} = \mathbf{L}_{\rm tot} + \mathbf{S}_{\rm tot}$, where $\mathbf{S}_{\rm tot} = \mathbf{S}_{\rm lt} + \frac{1}{2}$, and $\mathbf{L}_{\rm tot} = \mathbf{l}_\rho + \mathbf{l}_\lambda$ ($\mathbf{L}_{\rm tot} = \mathbf{l}_r$, for the quark-diquark model). The predicted masses, computed within the three-quark model, are shown in the third column, whereas their corresponding total strong decay widths are shown in the sixth column. The predicted masses, computed within the quark-diquark framework, are presented in the fourth column. Our theoretical results are compared with the experimental masses of the fifth column and the experimental decay widths of the seventh column taken from PDG [70] and Ref. [1]. The (*) indicate the experimental mass and decay width values included in the fits. The † indicates that there is no reported experimental mass or decay for that state. The †† indicates that there is no quark-diquark prediction for that state.

$\Omega_c(ssc)$ $\mathcal{F} = \mathbf{6}_{\rm f}$	$^{2S+1}L_J$	Three-quark predicted mass (MeV)	Quark-diquark predicted mass (MeV)	Experimental mass (MeV)	Predicted $\Gamma_{\rm tot}$ (MeV)	Experimental Γ (MeV)
$N = 0$						
$\vert l_\lambda = 0, l_\rho = 0, k_\lambda = 0, k_\rho = 0\rangle$	$^2S_{1/2}$	2709^{+10}_{-10}	2702^{+9}_{-9}	2695.0 ± 1.7 (*)	0	$< 10^{-7}$
$\vert l_\lambda = 0, l_\rho = 0, k_\lambda = 0, k_\rho = 0\rangle$	$^4S_{3/2}$	2778^{+9}_{-9}	2776^{+9}_{-9}	2765.9 ± 2.0 (*)	0	†
$N = 1$						
$\vert l_\lambda = 1, l_\rho = 0, k_\lambda = 0, k_\rho = 0\rangle$	$^2P_{1/2}$	3008^{+10}_{-10}	3000^{+9}_{-9}	3000.4 ± 0.22 (*)	4^{+2}_{-2}	$4.5 \pm 0.6 \pm 0.3$ (*)
$\vert l_\lambda = 1, l_\rho = 0, k_\lambda = 0, k_\rho = 0\rangle$	$^4P_{1/2}$	3050^{+15}_{-15}	3048^{+14}_{-14}	3050.2 ± 0.13	8^{+4}_{-4}	$0.8 \pm 0.2 \pm 0.1$
$\vert l_\lambda = 1, l_\rho = 0, k_\lambda = 0, k_\rho = 0\rangle$	$^2P_{3/2}$	3035^{+10}_{-10}	3025^{+10}_{-10}	3065.6 ± 0.28	26^{+13}_{-13}	$3.5 \pm 0.4 \pm 0.2$
$\vert l_\lambda = 1, l_\rho = 0, k_\lambda = 0, k_\rho = 0\rangle$	$^4P_{3/2}$	3077^{+9}_{-9}	3073^{+8}_{-8}	3090.2 ± 0.5	7^{+3}_{-3}	$8.7 \pm 1.0 \pm 0.8$
$\vert l_\lambda = 1, l_\rho = 0, k_\lambda = 0, k_\rho = 0\rangle$	$^4P_{5/2}$	3122^{+12}_{-12}	3115^{+12}_{-11}	3119.1 ± 1.0	50^{+25}_{-24}	2.6<
$\vert l_\lambda = 0, l_\rho = 1, k_\lambda = 0, k_\rho = 0\rangle$	$^2P_{1/2}$	3129^{+9}_{-9}	††	†	14^{+2}_{-10}	†
$\vert l_\lambda = 0, l_\rho = 1, k_\lambda = 0, k_\rho = 0\rangle$	$^2P_{3/2}$	3156^{+10}_{-10}	††	†	72^{+36}_{-35}	†
$N = 2$						
$\vert l_\lambda = 2, l_\rho = 0, k_\lambda = 0, k_\rho = 0\rangle$	$^2D_{3/2}$	3315^{+15}_{-14}	3306^{+14}_{-14}	†	11^{+5}_{-5}	†
$\vert l_\lambda = 2, l_\rho = 0, k_\lambda = 0, k_\rho = 0\rangle$	$^2D_{5/2}$	3360^{+17}_{-16}	3348^{+17}_{-17}	†	24^{+12}_{-12}	†
$\vert l_\lambda = 2, l_\rho = 0, k_\lambda = 0, k_\rho = 0\rangle$	$^4D_{1/2}$	3330^{+25}_{-25}	3328^{+24}_{-23}	†	16^{+8}_{-8}	†
$\vert l_\lambda = 2, l_\rho = 0, k_\lambda = 0, k_\rho = 0\rangle$	$^4D_{3/2}$	3357^{+18}_{-19}	3354^{+17}_{-17}	†	30^{+15}_{-15}	†
$\vert l_\lambda = 2, l_\rho = 0, k_\lambda = 0, k_\rho = 0\rangle$	$^4D_{5/2}$	3402^{+13}_{-13}	3396^{+12}_{-12}	†	62^{+31}_{-31}	†
$\vert l_\lambda = 2, l_\rho = 0, k_\lambda = 0, k_\rho = 0\rangle$	$^4D_{7/2}$	3466^{+23}_{-23}	3455^{+23}_{-23}	†	123^{+61}_{-62}	†
$\vert l_\lambda = 0, l_\rho = 0, k_\lambda = 1, k_\rho = 0\rangle$	$^2S_{1/2}$	3342^{+14}_{-14}	3331^{+15}_{-15}	†	2^{+1}_{-1}	†
$\vert l_\lambda = 0, l_\rho = 0, k_\lambda = 1, k_\rho = 0\rangle$	$^4S_{3/2}$	3411^{+13}_{-13}	3404^{+12}_{-12}	†	3^{+1}_{-1}	†
$\vert l_\lambda = 0, l_\rho = 0, k_\lambda = 0, k_\rho = 1\rangle$	$^2S_{1/2}$	3585^{+15}_{-15}	††	†	18^{+9}_{-9}	†
$\vert l_\lambda = 0, l_\rho = 0, k_\lambda = 0, k_\rho = 1\rangle$	$^4S_{3/2}$	3654^{+16}_{-16}	††	†	24^{+12}_{-12}	†
$\vert l_\lambda = 1, l_\rho = 1, k_\lambda = 0, k_\rho = 0\rangle$	$^2D_{3/2}$	3437^{+14}_{-14}	††	†	198^{+98}_{-98}	†
$\vert l_\lambda = 1, l_\rho = 1, k_\lambda = 0, k_\rho = 0\rangle$	$^2D_{5/2}$	3482^{+16}_{-16}	††	†	115^{+57}_{-56}	†
$\vert l_\lambda = 1, l_\rho = 1, k_\lambda = 0, k_\rho = 0\rangle$	$^2P_{1/2}$	3446^{+13}_{-13}	††	†	2^{+1}_{-1}	†
$\vert l_\lambda = 1, l_\rho = 1, k_\lambda = 0, k_\rho = 0\rangle$	$^2P_{3/2}$	3473^{+14}_{-14}	††	†	3^{+1}_{-1}	†
$\vert l_\lambda = 1, l_\rho = 1, k_\lambda = 0, k_\rho = 0\rangle$	$^2S_{1/2}$	3464^{+13}_{-13}	††	†	88^{+43}_{-44}	†
$\vert l_\lambda = 0, l_\rho = 2, k_\lambda = 0, k_\rho = 0\rangle$	$^2D_{3/2}$	3558^{+15}_{-15}	††	†	217^{+109}_{-107}	†
$\vert l_\lambda = 0, l_\rho = 2, k_\lambda = 0, k_\rho = 0\rangle$	$^2D_{5/2}$	3603^{+17}_{-17}	††	†	174^{+85}_{-86}	†
$\vert l_\lambda = 0, l_\rho = 2, k_\lambda = 0, k_\rho = 0\rangle$	$^4D_{1/2}$	3573^{+27}_{-26}	††	†	218^{+140}_{-139}	†
$\vert l_\lambda = 0, l_\rho = 2, k_\lambda = 0, k_\rho = 0\rangle$	$^4D_{3/2}$	3600^{+20}_{-20}	††	†	285^{+144}_{-145}	†
$\vert l_\lambda = 0, l_\rho = 2, k_\lambda = 0, k_\rho = 0\rangle$	$^4D_{5/2}$	3645^{+15}_{-16}	††	†	212^{+103}_{-104}	†
$\vert l_\lambda = 0, l_\rho = 2, k_\lambda = 0, k_\rho = 0\rangle$	$^4D_{7/2}$	3708^{+25}_{-25}	††	†	383^{+192}_{-194}	†

TABLE V. Same as Table IV, but for $\Sigma_c(nnc)$ states.

$\Sigma_c(nnc)$ $\mathcal{F} = \mathbf{6}_{\rm f}$	$^{2S+1}L_J$	Three-quark Predicted Mass (MeV)	Quark-diquark Predicted Mass (MeV)	Experimental Mass (MeV)	Predicted $\Gamma_{\rm tot}$ (MeV)	Experimental Γ (MeV)
$N = 0$						
$\vert l_\lambda = 0, l_\rho = 0, k_\lambda = 0, k_\rho = 0\rangle$	$^2S_{1/2}$	2456^{+11}_{-11}	2451^{+11}_{-11}	2453.5 ± 0.9 (*)	2^{+1}_{-1}	$2.3 \pm 0.3 \pm 0.3$ (*)
$\vert l_\lambda = 0, l_\rho = 0, k_\lambda = 0, k_\rho = 0\rangle$	$^4S_{3/2}$	2525^{+11}_{-11}	2524^{+11}_{-11}	2518.1 ± 2.8 (*)	15^{+8}_{-8}	$17.2 \pm 2.3 \pm 3.1$ (*)
$N = 1$						
$\vert l_\lambda = 1, l_\rho = 0, k_\lambda = 0, k_\rho = 0\rangle$	$^2P_{1/2}$	2811^{+12}_{-12}	2798^{+14}_{-14}	2800.0 ± 20.0 (*)	21^{+9}_{-8}	75 ± 60 (*)
$\vert l_\lambda = 1, l_\rho = 0, k_\lambda = 0, k_\rho = 0\rangle$	$^4P_{1/2}$	2853^{+17}_{-17}	2845^{+18}_{-18}	†	26^{+12}_{-13}	†
$\vert l_\lambda = 1, l_\rho = 0, k_\lambda = 0, k_\rho = 0\rangle$	$^2P_{3/2}$	2838^{+12}_{-13}	2823^{+15}_{-15}	†	86^{+40}_{-37}	†
$\vert l_\lambda = 1, l_\rho = 0, k_\lambda = 0, k_\rho = 0\rangle$	$^4P_{3/2}$	2880^{+13}_{-13}	2871^{+13}_{-13}	†	60^{+25}_{-19}	†
$\vert l_\lambda = 1, l_\rho = 0, k_\lambda = 0, k_\rho = 0\rangle$	$^4P_{5/2}$	2925^{+16}_{-16}	2913^{+16}_{-16}	†	164^{+95}_{-86}	†
$\vert l_\lambda = 0, l_\rho = 1, k_\lambda = 0, k_\rho = 0\rangle$	$^2P_{1/2}$	2994^{+16}_{-17}	††	†	125^{+61}_{-60}	†
$\vert l_\lambda = 0, l_\rho = 1, k_\lambda = 0, k_\rho = 0\rangle$	$^2P_{3/2}$	3021^{+17}_{-17}	††	†	125^{+63}_{-61}	†
$N = 2$						
$\vert l_\lambda = 2, l_\rho = 0, k_\lambda = 0, k_\rho = 0\rangle$	$^2D_{3/2}$	3175^{+17}_{-17}	3153^{+21}_{-21}	†	129^{+68}_{-69}	†
$\vert l_\lambda = 2, l_\rho = 0, k_\lambda = 0, k_\rho = 0\rangle$	$^2D_{5/2}$	3220^{+19}_{-19}	3195^{+23}_{-23}	†	216^{+124}_{-122}	†
$\vert l_\lambda = 2, l_\rho = 0, k_\lambda = 0, k_\rho = 0\rangle$	$^4D_{1/2}$	3190^{+28}_{-27}	3175^{+28}_{-28}	†	99^{+51}_{-51}	†
$\vert l_\lambda = 2, l_\rho = 0, k_\lambda = 0, k_\rho = 0\rangle$	$^4D_{3/2}$	3217^{+22}_{-22}	3201^{+23}_{-23}	†	155^{+76}_{-75}	†
$\vert l_\lambda = 2, l_\rho = 0, k_\lambda = 0, k_\rho = 0\rangle$	$^4D_{5/2}$	3262^{+18}_{-18}	3243^{+19}_{-20}	†	227^{+95}_{-94}	†
$\vert l_\lambda = 2, l_\rho = 0, k_\lambda = 0, k_\rho = 0\rangle$	$^4D_{7/2}$	3326^{+26}_{-26}	3302^{+28}_{-28}	†	385^{+214}_{-215}	†
$\vert l_\lambda = 0, l_\rho = 0, k_\lambda = 1, k_\rho = 0\rangle$	$^2S_{1/2}$	3202^{+17}_{-17}	3178^{+21}_{-21}	†	8^{+3}_{-3}	†
$\vert l_\lambda = 0, l_\rho = 0, k_\lambda = 1, k_\rho = 0\rangle$	$^4S_{3/2}$	3271^{+18}_{-18}	3251^{+20}_{-20}	†	7^{+3}_{-3}	†
$\vert l_\lambda = 0, l_\rho = 0, k_\lambda = 0, k_\rho = 1\rangle$	$^2S_{1/2}$	3567^{+31}_{-31}	††	†	19^{+10}_{-9}	†
$\vert l_\lambda = 0, l_\rho = 0, k_\lambda = 0, k_\rho = 1\rangle$	$^4S_{3/2}$	3637^{+33}_{-33}	††	†	26^{+13}_{-13}	†
$\vert l_\lambda = 1, l_\rho = 1, k_\lambda = 0, k_\rho = 0\rangle$	$^2D_{3/2}$	3358^{+22}_{-23}	††	†	386^{+189}_{-189}	†
$\vert l_\lambda = 1, l_\rho = 1, k_\lambda = 0, k_\rho = 0\rangle$	$^2D_{5/2}$	3403^{+24}_{-24}	††	†	334^{+174}_{-172}	†
$\vert l_\lambda = 1, l_\rho = 1, k_\lambda = 0, k_\rho = 0\rangle$	$^2P_{1/2}$	3367^{+22}_{-22}	††	†	8^{+6}_{-6}	†
$\vert l_\lambda = 1, l_\rho = 1, k_\lambda = 0, k_\rho = 0\rangle$	$^2P_{3/2}$	3394^{+23}_{-23}	††	†	32^{+29}_{-28}	†
$\vert l_\lambda = 1, l_\rho = 1, k_\lambda = 0, k_\rho = 0\rangle$	$^2S_{1/2}$	3385^{+22}_{-23}	††	†	100^{+52}_{-52}	†
$\vert l_\lambda = 0, l_\rho = 2, k_\lambda = 0, k_\rho = 0\rangle$	$^2D_{3/2}$	3540^{+31}_{-31}	††	†	476^{+229}_{-226}	†
$\vert l_\lambda = 0, l_\rho = 2, k_\lambda = 0, k_\rho = 0\rangle$	$^2D_{5/2}$	3585^{+32}_{-32}	††	†	722^{+369}_{-371}	†
$\vert l_\lambda = 0, l_\rho = 2, k_\lambda = 0, k_\rho = 0\rangle$	$^4D_{1/2}$	3555^{+39}_{-39}	††	†	1150^{+565}_{-558}	†
$\vert l_\lambda = 0, l_\rho = 2, k_\lambda = 0, k_\rho = 0\rangle$	$^4D_{3/2}$	3582^{+35}_{-35}	††	†	652^{+319}_{-313}	†
$\vert l_\lambda = 0, l_\rho = 2, k_\lambda = 0, k_\rho = 0\rangle$	$^4D_{5/2}$	3627^{+33}_{-33}	††	†	412^{+207}_{-206}	†
$\vert l_\lambda = 0, l_\rho = 2, k_\lambda = 0, k_\rho = 0\rangle$	$^4D_{7/2}$	3691^{+38}_{-38}	††	†	1879^{+977}_{-974}	†

A. Assignments of charmed baryons

First, we discuss our assignments based on our theoretical analyses of the charmed baryons Ω_c, Ξ'_c, Σ_c, Ξ_c, and Λ_c. As a first criterion, we use our mass spectrum to identify the charmed baryon resonances, and the decay width as a secondary criterion. The classification for the quark-diquark model is equivalent to that of the three-quark model when we describe ground states and λ-type excitations. When states are identified as ρ-type excitations in the three-quark model, there are no equivalent states in the quark-diquark model (see Tables IV–VIII).

1. Ω_c

Our results for the Ω_c resonances are reported in Table IV; they are in good agreement with the experimental masses reported in the PDG. Our results are also consistent with our previous calculations [55]. Here we have extended our calculations up to D-wave states. The Ω_c and $\Omega_c(2770)$ states are well reproduced [9] in our model. They are identified as the ground states with quantum numbers (QN) $J^P = 1/2^+$ and $J^P = 3/2^+$; note that these QN have not been yet measured however they have been identified by quark model predictions [9]. The observed $\Omega_c(3000)$ [1,2]

TABLE VI. Same as Table IV, but for $\Xi'_c(snc)$ states.

$\Xi'_c(snc)$ $\mathcal{F} = \mathbf{6}_{\rm f}$	${}^{2S+1}L_J$	Three-quark predicted mass (MeV)	Quark-diquark predicted mass (MeV)	Experimental mass (MeV)	Predicted $\Gamma_{\rm tot}$ (MeV)	Experimental Γ (MeV)
$N = 0$						
$\vert l_\lambda = 0, l_\rho = 0, k_\lambda = 0, k_\rho = 0\rangle$	${}^2S_{1/2}$	2571^{+8}_{-8}	2577^{+10}_{-10}	2578.0 ± 0.9 (*)	0	†
$\vert l_\lambda = 0, l_\rho = 0, k_\lambda = 0, k_\rho = 0\rangle$	${}^4S_{3/2}$	2640^{+7}_{-7}	2650^{+9}_{-9}	2645.9 ± 0.71 (*)	$0.4^{+0.2}_{-0.2}$	2.25 ± 0.41 (*)
$N = 1$						
$\vert l_\lambda = 1, l_\rho = 0, k_\lambda = 0, k_\rho = 0\rangle$	${}^2P_{1/2}$	2893^{+9}_{-9}	2893^{+11}_{-11}	†	7^{+4}_{-3}	†
$\vert l_\lambda = 1, l_\rho = 0, k_\lambda = 0, k_\rho = 0\rangle$	${}^4P_{1/2}$	2935^{+14}_{-15}	2941^{+14}_{-14}	2923.0 ± 0.35	5^{+2}_{-3}	7.1 ± 2.0
$\vert l_\lambda = 1, l_\rho = 0, k_\lambda = 0, k_\rho = 0\rangle$	${}^2P_{3/2}$	2920^{+9}_{-9}	2919^{+13}_{-13}	2938.5 ± 0.3	28^{+14}_{-14}	15 ± 9
$\vert l_\lambda = 1, l_\rho = 0, k_\lambda = 0, k_\rho = 0\rangle$	${}^4P_{3/2}$	2962^{+9}_{-9}	2966^{+10}_{-10}	2964.9 ± 0.33 (*)	19^{+9}_{-9}	14.1 ± 1.6 (*)
$\vert l_\lambda = 1, l_\rho = 0, k_\lambda = 0, k_\rho = 0\rangle$	${}^4P_{5/2}$	3007^{+12}_{-12}	3009^{+14}_{-14}	†	43^{+21}_{-21}	†
$\vert l_\lambda = 0, l_\rho = 1, k_\lambda = 0, k_\rho = 0\rangle$	${}^2P_{1/2}$	3040^{+10}_{-9}	††	3055.9 ± 0.4 (*)	157^{+80}_{-80}	7.8 ± 1.9 (*)
$\vert l_\lambda = 0, l_\rho = 1, k_\lambda = 0, k_\rho = 0\rangle$	${}^2P_{3/2}$	3067^{+10}_{-10}	††	3078.6 ± 2.8 (*)	100^{+47}_{-48}	4.6 ± 3.3 (*)
$N = 2$						
$\vert l_\lambda = 2, l_\rho = 0, k_\lambda = 0, k_\rho = 0\rangle$	${}^2D_{3/2}$	3223^{+14}_{-14}	3218^{+17}_{-17}	†	20^{+10}_{-10}	†
$\vert l_\lambda = 2, l_\rho = 0, k_\lambda = 0, k_\rho = 0\rangle$	${}^2D_{5/2}$	3268^{+16}_{-16}	3261^{+21}_{-20}	†	64^{+32}_{-33}	†
$\vert l_\lambda = 2, l_\rho = 0, k_\lambda = 0, k_\rho = 0\rangle$	${}^4D_{1/2}$	3238^{+25}_{-25}	3239^{+23}_{-24}	†	29^{+15}_{-15}	†
$\vert l_\lambda = 2, l_\rho = 0, k_\lambda = 0, k_\rho = 0\rangle$	${}^4D_{3/2}$	3265^{+19}_{-19}	3265^{+18}_{-18}	†	53^{+26}_{-26}	†
$\vert l_\lambda = 2, l_\rho = 0, k_\lambda = 0, k_\rho = 0\rangle$	${}^4D_{5/2}$	3310^{+13}_{-13}	3308^{+15}_{-14}	†	97^{+46}_{-47}	†
$\vert l_\lambda = 2, l_\rho = 0, k_\lambda = 0, k_\rho = 0\rangle$	${}^4D_{7/2}$	3373^{+23}_{-23}	3368^{+25}_{-25}	†	161^{+80}_{-80}	†
$\vert l_\lambda = 0, l_\rho = 0, k_\lambda = 1, k_\rho = 0\rangle$	${}^2S_{1/2}$	3250^{+13}_{-14}	3244^{+18}_{-18}	†	2^{+1}_{-1}	†
$\vert l_\lambda = 0, l_\rho = 0, k_\lambda = 1, k_\rho = 0\rangle$	${}^4S_{3/2}$	3319^{+14}_{-14}	3316^{+15}_{-15}	†	5^{+2}_{-2}	†
$\vert l_\lambda = 0, l_\rho = 0, k_\lambda = 0, k_\rho = 1\rangle$	${}^2S_{1/2}$	3544^{+19}_{-19}	††	†	21^{+10}_{-10}	†
$\vert l_\lambda = 0, l_\rho = 0, k_\lambda = 0, k_\rho = 1\rangle$	${}^4S_{3/2}$	3613^{+20}_{-21}	††	†	29^{+14}_{-14}	†
$\vert l_\lambda = 1, l_\rho = 1, k_\lambda = 0, k_\rho = 0\rangle$	${}^2D_{3/2}$	3370^{+15}_{-15}	††	†	229^{+112}_{-111}	†
$\vert l_\lambda = 1, l_\rho = 1, k_\lambda = 0, k_\rho = 0\rangle$	${}^2D_{5/2}$	3415^{+17}_{-17}	††	†	134^{+67}_{-66}	†
$\vert l_\lambda = 1, l_\rho = 1, k_\lambda = 0, k_\rho = 0\rangle$	${}^2P_{1/2}$	3379^{+14}_{-14}	††	†	3^{+1}_{-1}	†
$\vert l_\lambda = 1, l_\rho = 1, k_\lambda = 0, k_\rho = 0\rangle$	${}^2P_{3/2}$	3406^{+16}_{-16}	††	†	3^{+1}_{-1}	†
$\vert l_\lambda = 1, l_\rho = 1, k_\lambda = 0, k_\rho = 0\rangle$	${}^2S_{1/2}$	3397^{+15}_{-15}	††	†	56^{+28}_{-28}	†
$\vert l_\lambda = 0, l_\rho = 2, k_\lambda = 0, k_\rho = 0\rangle$	${}^2D_{3/2}$	3517^{+19}_{-18}	††	†	319^{+153}_{-158}	†
$\vert l_\lambda = 0, l_\rho = 2, k_\lambda = 0, k_\rho = 0\rangle$	${}^2D_{5/2}$	3563^{+21}_{-21}	††	†	232^{+116}_{-115}	†
$\vert l_\lambda = 0, l_\rho = 2, k_\lambda = 0, k_\rho = 0\rangle$	${}^4D_{1/2}$	3532^{+29}_{-29}	††	†	632^{+332}_{-330}	†
$\vert l_\lambda = 0, l_\rho = 2, k_\lambda = 0, k_\rho = 0\rangle$	${}^4D_{3/2}$	3559^{+23}_{-23}	††	†	452^{+221}_{-223}	†
$\vert l_\lambda = 0, l_\rho = 2, k_\lambda = 0, k_\rho = 0\rangle$	${}^4D_{5/2}$	3604^{+20}_{-20}	††	†	208^{+99}_{-99}	†
$\vert l_\lambda = 0, l_\rho = 2, k_\lambda = 0, k_\rho = 0\rangle$	${}^4D_{7/2}$	3668^{+28}_{-28}	††	†	578^{+293}_{-297}	†

resonance could be identified as a P_λ-wave state with $J^P = 1/2^-$, where the total-internal-spin is $S = 1/2$; our theoretical width is compatible with the experimental value. Our assignment of $\Omega_c(3000)$ is supported by lattice QCD calculations [71], and is also compatible with diquark model interpretations of Ref. [72], and predictions of QCD sum rule approaches [73]. The $\Omega_c(3050)$ has an excellent match in our model; the mass is well reproduced, but the width is slightly overestimated; the $\Omega_c(3050)$ is identified as the $J^P = 1/2^-$ state, with total-internal-spin $S = 3/2$. Our assignment for $\Omega_c(3050)$ is likewise supported by Refs. [71–73], but it also has been identified as a $J^P = 3/2^-$ state, see. Ref. [43]. In our calculations, the central value deviates 20 MeV for $\Omega_c(3065)$; however, the width is overestimated. Hence, we identify the observed $\Omega_c(3065)$ as the state $J^P = 3/2^-$ with internal-total-spin $S = 1/2$. It should be noted that our state $J^P = 3/2^-$ is lighter in mass that the state $J^P = 1/2^-$; this may be a numerical consequence of the fit. However, this opens the possibility of interchanging the assignments of the $\Omega_c(3050)$ and $\Omega_c(3065)$ states, with $J^P = 3/2^-$ and $J^P = 1/2^-$, respectively. The identification of $\Omega_c(3050)$ as a $J^P = 3/2^-$ state is supported by Refs. [43,71–73]. Only future experiments will confirm the right order and the assignments. The $\Omega_c(3090)$ is identified as the state $J^P = 3/2^-$ with spin $S = 3/2$; however, its theoretical

TABLE VII. Same as Table IV, but for $\Xi_c(snc)$ states.

$\Xi_c(snc)$ $\bar{\mathbf{3}}_{\rm f}$	$^{2S+1}L_J$	Three-quark predicted mass (MeV)	Quark-diquark predicted mass (MeV)	Experimental mass (MeV)	Predicted $\Gamma_{\rm tot}$ (MeV)	Experimental Γ (MeV)
$N=0$						
$\vert l_\lambda=0, l_\rho=0, k_\lambda=0, k_\rho=0\rangle$	$^2S_{1/2}$	2466^{+10}_{-10}	2473^{+10}_{-10}	2469.42 ± 1.77 (*)	0	≈0
$N=1$						
$\vert l_\lambda=1, l_\rho=0, k_\lambda=0, k_\rho=0\rangle$	$^2P_{1/2}$	2788^{+10}_{-10}	2789^{+9}_{-9}	2793.3 ± 0.28 (*)	3^{+2}_{-2}	9.5 ± 2.0 (*)
$\vert l_\lambda=1, l_\rho=0, k_\lambda=0, k_\rho=0\rangle$	$^2P_{3/2}$	2815^{+10}_{-10}	2814^{+9}_{-9}	2818.49 ± 2.07 (*)	5^{+2}_{-2}	2.48 ± 0.5 (*)
$\vert l_\lambda=0, l_\rho=1, k_\lambda=0, k_\rho=0\rangle$	$^2P_{1/2}$	2935^{+12}_{-12}	††	†	17^{+9}_{-8}	†
$\vert l_\lambda=0, l_\rho=1, k_\lambda=0, k_\rho=0\rangle$	$^4P_{1/2}$	2977^{+20}_{-20}	††	2968.6 ± 3.3	13^{+6}_{-6}	20 ± 3.5
$\vert l_\lambda=0, l_\rho=1, k_\lambda=0, k_\rho=0\rangle$	$^2P_{3/2}$	2962^{+12}_{-12}	††	†	89^{+45}_{-45}	†
$\vert l_\lambda=0, l_\rho=1, k_\lambda=0, k_\rho=0\rangle$	$^4P_{3/2}$	3004^{+17}_{-17}	††	†	56^{+29}_{-31}	†
$\vert l_\lambda=0, l_\rho=1, k_\lambda=0, k_\rho=0\rangle$	$^4P_{5/2}$	3049^{+18}_{-19}	††	†	122^{+59}_{-60}	†
$N=2$						
$\vert l_\lambda=2, l_\rho=0, k_\lambda=0, k_\rho=0\rangle$	$^2D_{3/2}$	3118^{+14}_{-14}	3113^{+14}_{-14}	3122.9 ± 1.23	50^{+24}_{-25}	4 ± 4
$\vert l_\lambda=2, l_\rho=0, k_\lambda=0, k_\rho=0\rangle$	$^2D_{5/2}$	3164^{+16}_{-16}	3156^{+16}_{-16}	†	132^{+63}_{-64}	†
$\vert l_\lambda=0, l_\rho=0, k_\lambda=1, k_\rho=0\rangle$	$^2S_{1/2}$	3145^{+14}_{-13}	3139^{+13}_{-14}	†	5^{+2}_{-2}	†
$\vert l_\lambda=0, l_\rho=0, k_\lambda=0, k_\rho=1\rangle$	$^2S_{1/2}$	3440^{+20}_{-20}	††	†	7^{+3}_{-3}	†
$\vert l_\lambda=1, l_\rho=1, k_\lambda=0, k_\rho=0\rangle$	$^2D_{3/2}$	3265^{+16}_{-16}	††	†	54^{+26}_{-27}	†
$\vert l_\lambda=1, l_\rho=1, k_\lambda=0, k_\rho=0\rangle$	$^2D_{5/2}$	3311^{+17}_{-18}	††	†	119^{+57}_{-58}	†
$\vert l_\lambda=1, l_\rho=1, k_\lambda=0, k_\rho=0\rangle$	$^4D_{1/2}$	3280^{+29}_{-29}	††	†	24^{+12}_{-12}	†
$\vert l_\lambda=1, l_\rho=1, k_\lambda=0, k_\rho=0\rangle$	$^4D_{3/2}$	3307^{+23}_{-23}	††	†	92^{+46}_{-46}	†
$\vert l_\lambda=1, l_\rho=1, k_\lambda=0, k_\rho=0\rangle$	$^4D_{5/2}$	3353^{+19}_{-19}	††	†	153^{+75}_{-75}	†
$\vert l_\lambda=1, l_\rho=1, k_\lambda=0, k_\rho=0\rangle$	$^4D_{7/2}$	3416^{+26}_{-27}	††	†	194^{+97}_{-96}	†
$\vert l_\lambda=1, l_\rho=1, k_\lambda=0, k_\rho=0\rangle$	$^2P_{1/2}$	3274^{+15}_{-15}	††	†	$0.4^{+0.2}_{-0.2}$	†
$\vert l_\lambda=1, l_\rho=1, k_\lambda=0, k_\rho=0\rangle$	$^2P_{3/2}$	3302^{+16}_{-16}	††	†	2^{+1}_{-1}	†
$\vert l_\lambda=1, l_\rho=1, k_\lambda=0, k_\rho=0\rangle$	$^4P_{1/2}$	3316^{+22}_{-22}	††	†	$0.3^{+0.1}_{-0.1}$	†
$\vert l_\lambda=1, l_\rho=1, k_\lambda=0, k_\rho=0\rangle$	$^4P_{3/2}$	3344^{+19}_{-19}	††	†	$1.4^{+0.7}_{-0.7}$	†
$\vert l_\lambda=1, l_\rho=1, k_\lambda=0, k_\rho=0\rangle$	$^4P_{5/2}$	3389^{+21}_{-22}	††	†	4^{+2}_{-2}	†
$\vert l_\lambda=1, l_\rho=1, k_\lambda=0, k_\rho=0\rangle$	$^4S_{3/2}$	3362^{+19}_{-19}	††	†	36^{+18}_{-18}	†
$\vert l_\lambda=1, l_\rho=1, k_\lambda=0, k_\rho=0\rangle$	$^2S_{1/2}$	3293^{+15}_{-15}	††	†	30^{+15}_{-15}	†
$\vert l_\lambda=0, l_\rho=2, k_\lambda=0, k_\rho=0\rangle$	$^2D_{3/2}$	3413^{+20}_{-20}	††	†	133^{+64}_{-64}	†
$\vert l_\lambda=0, l_\rho=2, k_\lambda=0, k_\rho=0\rangle$	$^2D_{5/2}$	3458^{+22}_{-22}	††	†	119^{+59}_{-59}	†

mass is slightly underestimated, but the theoretical width is in good agreement with the experimental value. The $\Omega_c(3090)$ assignment is compatible with the predictions of Refs. [71–73], but also has been identified as a $J^P = 5/2^-$ state, see Ref. [43]. Finally, the mass of the $\Omega_c(3120)$ resonance is well reproduced in our model; it is identified as the state $J^P = 5/2^-$ with spin $S = 3/2$. This state was not confirmed by Belle [2], other interpretations are therefore possible. Since this state is very narrow, it can be described as a molecular state [55]. The identification of $\Omega_c(3120)$ as $J^P = 5/2^-$ is supported by Refs. [71–73], but this picture could not be confirmed by the recent LHCb analysis [74]. In the present work the identifications of the $\Omega_c(3000)$ and $\Omega_c(3050)$ are predicted to have $J^P = 1/2^-$. The $\Omega_c(3066)$ and $\Omega_c(3090)$ both are selected to have $J^P = 3/2^-$, and the $\Omega_c(3119)$ is possibly a $J^P = 5/2^-$ state in accordance with Refs. [71–73]. Nevertheless, other interpretations were proposed in Refs. [42,43] based on the constituent quark model: the $\Omega_c(3000)$, $\Omega_c(3050)$, $\Omega_c(3066)$, and $\Omega_c(3090)$ are $\Omega_c(1P)$ states are predicted to have $J^P = 1/2^-$, $3/2^-$, $3/2^-$, and $5/2^-$ respectively. The $\Omega_c(3119)$ may correspond to one of the two $\Omega_c(2S)$ states.

2. Σ_c

Our results for Σ_c states are reported in Table V. There are only three experimentally observed Σ_c states, all of which have masses that are in excellent agreement with our predictions. $\Sigma_c(2455)$ is identified as the ground state $J^P = 1/2^+$. The quantum numbers have not yet been measured, and our predicted masses and decay widths are in good agreement with the experimental data. We find

TABLE VIII. Same as Table IV, but for $\Lambda_c(nnc)$ states.

$\Lambda_c(nnc)$ $\bar{\mathbf{3}}_{\mathrm{f}}$	$^{2S+1}L_J$	Three-quark predicted mass (MeV)	Quark-diquark predicted mass (MeV)	Experimental mass (MeV)	Predicted Γ_{tot} (MeV)	Experimental Γ (MeV)
$N = 0$						
$\vert l_\lambda = 0, l_\rho = 0, k_\lambda = 0, k_\rho = 0\rangle$	$^2S_{1/2}$	2261^{+11}_{-11}	2264^{+10}_{-10}	2286.5 ± 0.14 (*)	0	≈0
$N = 1$						
$\vert l_\lambda = 1, l_\rho = 0, k_\lambda = 0, k_\rho = 0\rangle$	$^2P_{1/2}$	2616^{+10}_{-10}	2611^{+9}_{-9}	2592.3 ± 0.28 (*)	2^{+1}_{-1}	2.6 ± 0.6 (*)
$\vert l_\lambda = 1, l_\rho = 0, k_\lambda = 0, k_\rho = 0\rangle$	$^2P_{3/2}$	2643^{+10}_{-10}	2636^{+9}_{-9}	2625.0 ± 0.18 (*)	10^{+5}_{-5}	< 0.97
$\vert l_\lambda = 0, l_\rho = 1, k_\lambda = 0, k_\rho = 0\rangle$	$^2P_{1/2}$	2799^{+15}_{-15}	††	†	60^{+27}_{-28}	†
$\vert l_\lambda = 0, l_\rho = 1, k_\lambda = 0, k_\rho = 0\rangle$	$^4P_{1/2}$	2841^{+23}_{-23}	††	†	33^{+16}_{-16}	†
$\vert l_\lambda = 0, l_\rho = 1, k_\lambda = 0, k_\rho = 0\rangle$	$^2P_{3/2}$	2826^{+15}_{-15}	††	†	93^{+45}_{-46}	†
$\vert l_\lambda = 0, l_\rho = 1, k_\lambda = 0, k_\rho = 0\rangle$	$^4P_{3/2}$	2868^{+20}_{-20}	††	†	122^{+59}_{-59}	†
$\vert l_\lambda = 0, l_\rho = 1, k_\lambda = 0, k_\rho = 0\rangle$	$^4P_{5/2}$	2913^{+21}_{-21}	††	†	108^{+52}_{-53}	†
$N = 2$						
$\vert l_\lambda = 2, l_\rho = 0, k_\lambda = 0, k_\rho = 0\rangle$	$^2D_{3/2}$	2980^{+14}_{-14}	2967^{+14}_{-14}	2856.1 ± 6	70^{+34}_{-34}	68 ± 22
$\vert l_\lambda = 2, l_\rho = 0, k_\lambda = 0, k_\rho = 0\rangle$	$^2D_{5/2}$	3025^{+15}_{-15}	3009^{+16}_{-16}	2881.63 ± 0.24	171^{+84}_{-83}	5.6 ± 0.8
$\vert l_\lambda = 0, l_\rho = 0, k_\lambda = 1, k_\rho = 0\rangle$	$^2S_{1/2}$	3007^{+13}_{-13}	2992^{+14}_{-14}	2766 ± 2.4	5^{+3}_{-3}	50
$\vert l_\lambda = 0, l_\rho = 0, k_\lambda = 0, k_\rho = 1\rangle$	$^2S_{1/2}$	3372^{+29}_{-29}	††	†	6^{+3}_{-3}	†
$\vert l_\lambda = 1, l_\rho = 1, k_\lambda = 0, k_\rho = 0\rangle$	$^2D_{3/2}$	3163^{+20}_{-20}	††	†	70^{+34}_{-34}	†
$\vert l_\lambda = 1, l_\rho = 1, k_\lambda = 0, k_\rho = 0\rangle$	$^2D_{5/2}$	3208^{+21}_{-21}	††	†	133^{+65}_{-65}	†
$\vert l_\lambda = 1, l_\rho = 1, k_\lambda = 0, k_\rho = 0\rangle$	$^4D_{1/2}$	3178^{+33}_{-32}	††	†	34^{+17}_{-17}	†
$\vert l_\lambda = 1, l_\rho = 1, k_\lambda = 0, k_\rho = 0\rangle$	$^4D_{3/2}$	3205^{+28}_{-27}	††	†	106^{+50}_{-52}	†
$\vert l_\lambda = 1, l_\rho = 1, k_\lambda = 0, k_\rho = 0\rangle$	$^4D_{5/2}$	3250^{+24}_{-24}	††	†	163^{+80}_{-79}	†
$\vert l_\lambda = 1, l_\rho = 1, k_\lambda = 0, k_\rho = 0\rangle$	$^4D_{7/2}$	3313^{+30}_{-30}	††	†	230^{+118}_{-116}	†
$\vert l_\lambda = 1, l_\rho = 1, k_\lambda = 0, k_\rho = 0\rangle$	$^2P_{1/2}$	3172^{+20}_{-20}	††	†	$0.5^{+0.3}_{-0.3}$	†
$\vert l_\lambda = 1, l_\rho = 1, k_\lambda = 0, k_\rho = 0\rangle$	$^2P_{3/2}$	3199^{+20}_{-20}	††	†	2^{+1}_{-1}	†
$\vert l_\lambda = 1, l_\rho = 1, k_\lambda = 0, k_\rho = 0\rangle$	$^4P_{1/2}$	3214^{+26}_{-26}	††	†	$0.3^{+0.2}_{-0.2}$	†
$\vert l_\lambda = 1, l_\rho = 1, k_\lambda = 0, k_\rho = 0\rangle$	$^4P_{3/2}$	3241^{+24}_{-24}	††	†	$1.5^{+0.7}_{-0.7}$	†
$\vert l_\lambda = 1, l_\rho = 1, k_\lambda = 0, k_\rho = 0\rangle$	$^4P_{5/2}$	3286^{+26}_{-26}	††	†	4^{+2}_{-2}	†
$\vert l_\lambda = 1, l_\rho = 1, k_\lambda = 0, k_\rho = 0\rangle$	$^4S_{3/2}$	3259^{+24}_{-24}	††	†	32^{+16}_{-16}	†
$\vert l_\lambda = 1, l_\rho = 1, k_\lambda = 0, k_\rho = 0\rangle$	$^2S_{1/2}$	3190^{+20}_{-20}	††	†	30^{+15}_{-15}	†
$\vert l_\lambda = 0, l_\rho = 2, k_\lambda = 0, k_\rho = 0\rangle$	$^2D_{3/2}$	3345^{+30}_{-30}	††	†	154^{+75}_{-74}	†
$\vert l_\lambda = 0, l_\rho = 2, k_\lambda = 0, k_\rho = 0\rangle$	$^2D_{5/2}$	3390^{+30}_{-30}	††	†	202^{+102}_{-102}	†

a similar situation in the case of $\Sigma_c(2520)$, which is identified as a ground state with a spin excitation $J^P = 3/2^+$. The quantum numbers have not yet been measured, but our theoretical mass is in good agreement with the experimental data, and the decay width is well reproduced. $\Sigma_c(2800)$ is identified as the first P_λ-wave excitation, with the assignment $J^P = 1/2^-$; the theoretical mass and width are compatible with the experimental data. The lack of data limits the identification of the Σ_c states. For instance, Ref. [75] utilizes the chiral quark model to identify the $\Sigma_c(2800)$ as two overlapping P-wave Σ_c resonances with $J^P = 3/2^-$ and $J^P = 5/2^-$, respectively.

3. Ξ_c' and Ξ_c

Our results for Ξ_c' resonances are reported in Table VI and those for Ξ_c are reported in Table VII. The Ξ_c' states belong to the sextet configuration and the Ξ_c states belong to the anti-3-plet. Identifying the available data for these states is more complex, since there are several theoretical excited states for Ξ_c' and Ξ_c in the same energy region. Additionally, for these states some experimental data are puzzling, as Ref. [3] reports a state with a central mass close to 2965 MeV. Hence, further studies are required in order to establish whether this narrow resonance is a different baryon from the narrow resonance at 2970 MeV found by Belle [6]. Moreover, the Belle collaboration recently measured the quantum numbers of $\Xi_c^+(2970)$ to be $J^P = 1/2^+$ [11], which could indicate that this state is a radial excitation. The Ξ_c' and Ξ_c ground states are well reproduced in our model, and are identified as $J^P = 1/2^+$ of the sextet and anti-3-plet, respectively. $\Xi_c(2645)$ is identified as the $J^P = 3/2^+$ member of the sextet. In our

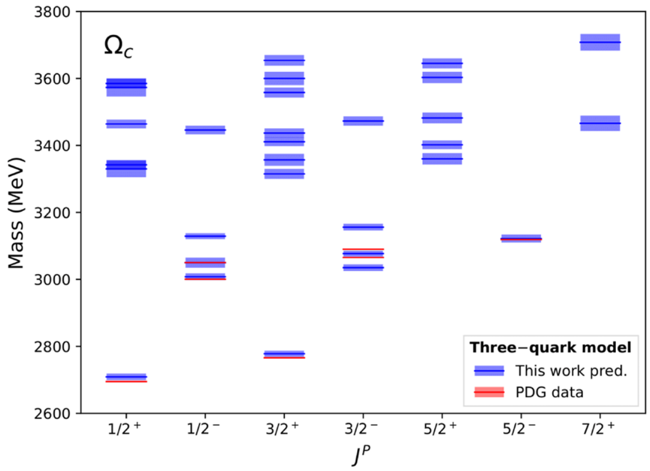

FIG. 2. Ω_c mass spectra and tentative quantum number assignments based on the three-quark model Hamiltonian of Eqs. (1) and (2). The theoretical predictions and their uncertainties (blue lines and bands) are compared with the experimental results (red lines and bands) reported in the PDG [9]. The experimental errors are too small to be evaluated on this energy scale.

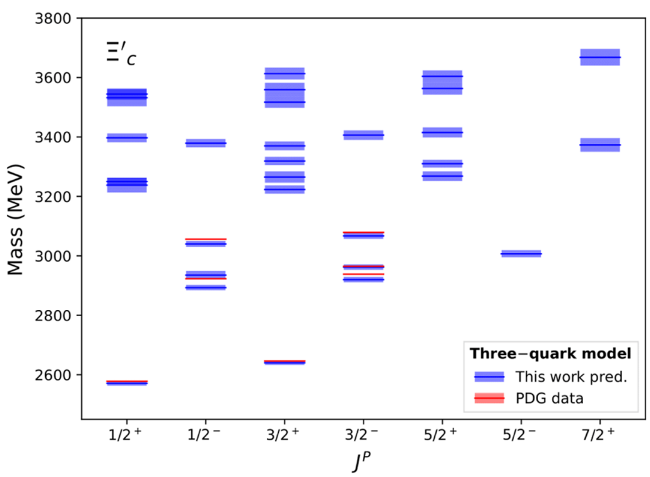

FIG. 3. Same as Fig. 2, but for Ξ'_c states.

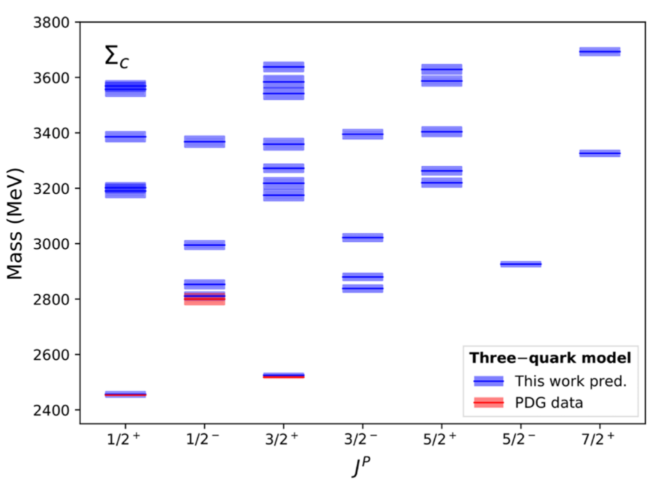

FIG. 4. Same as Fig. 2, but for Σ_c states.

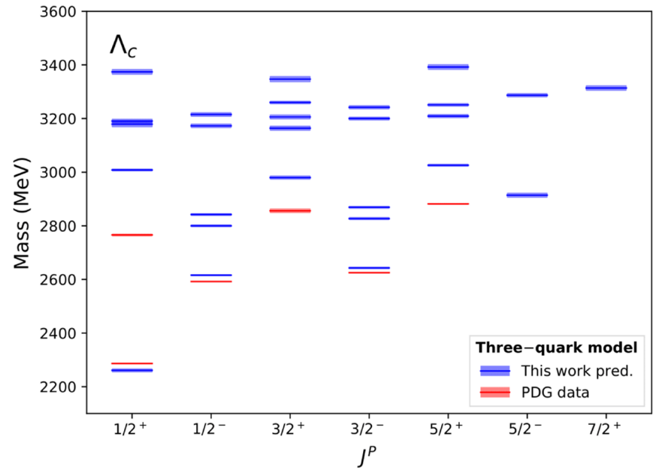

FIG. 5. Same as Fig. 2, but for Λ_c states.

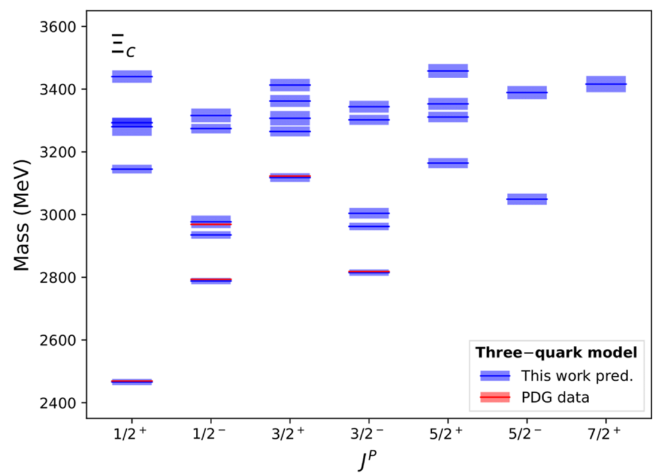

FIG. 6. Same as Fig. 2, but for Ξ_c states.

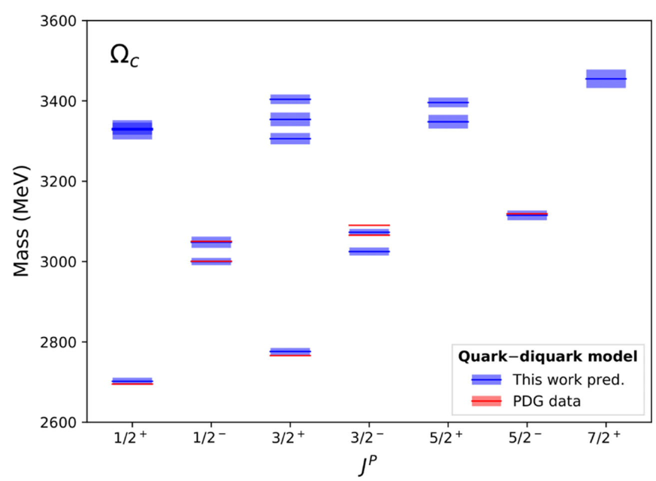

FIG. 7. Ω_c mass spectra and tentative quantum number assignments based on the quark-diquark model Hamiltonian of Eqs. (1) and (4). The theoretical predictions and their uncertainties (blue lines and bands) are compared with the experimental results (red lines and bands) reported in the PDG [9]. The experimental errors are too small to be evaluated on this energy scale.

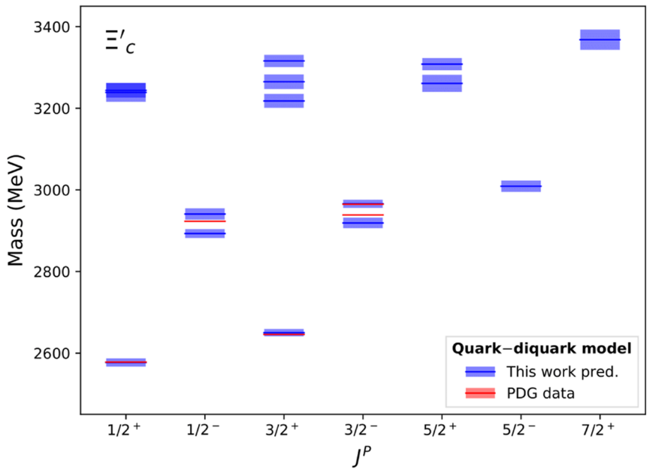

FIG. 8. Same as Fig. 7, but for Ξ_c' states.

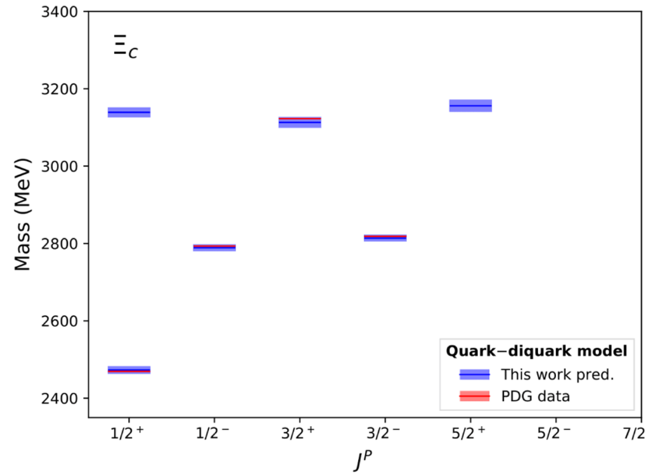

FIG. 11. Same as Fig. 7, but for Ξ_c states.

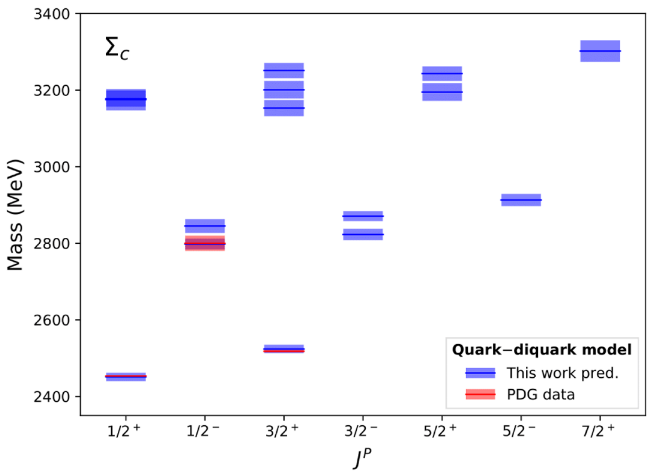

FIG. 9. Same as Fig. 7, but for Σ_c states.

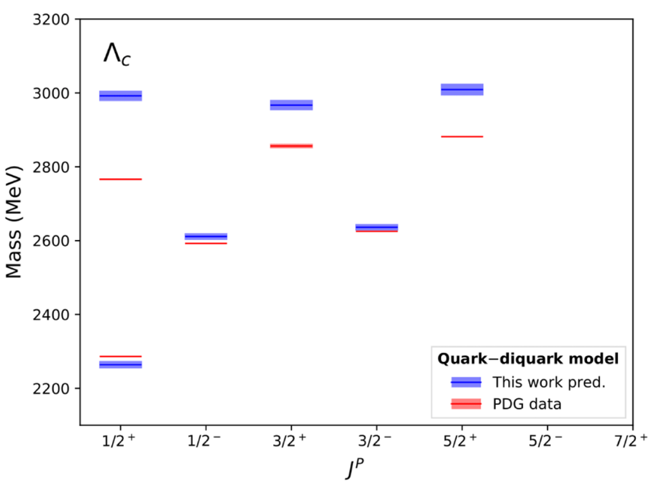

FIG. 10. Same as Fig. 7, but for Λ_c states.

model, its mass is well reproduced and the width is underestimated. The $\Xi_c(2790)$ and $\Xi_c(2815)$ states are identified as $J^P = 1/2^-$ and $J^P = 3/2^-$ respectively, see Table VII; these quantum numbers, which have not yet been measured, refer to the first orbital excitations of the anti-3-plet states. $\Xi_c(2923)$ is identified as the P_λ-wave excitation $J^P = 1/2^-$ with spin $S = 3/2$ that belongs to the sextet ($\Xi_c'(1P)$ states); the theoretical width is compatible with the experimental value. The assignment of $\Xi_c(2923)$ as $J^P = 1/2^-$ is consistent with our previous work [56] and supported by the QCD sum rule approaches in Refs. [24,76]; although in Ref. [77] it is identified as a $J^P = 3/2^-$ state. The $\Xi_c(2930)$ is identified as a P_λ-wave $J^P = 3/2^-$ state with $S = 1/2$ that belongs to the sextet; our theoretical mass deviates by 5 MeV, but our theoretical width is in good agreement with the experimental value. The assignment of $\Xi_c(2930)$ as $J^P = 3/2^-$ state is supported by several approaches [24,56,76,77]. However, there is another possible assignment to this resonance, as the $J^P = 1/2^-$ state with $S = 1/2$ is close in mass, and belongs to the anti-3-plet; only future experiments will determine the correct assignment.

Furthermore, there is a puzzle regarding the state observed by LHCb [3]: it has not been established whether the $\Xi_c^0(2965)$ state is the isospin partner of $\Xi_c^+(2970)$, or a different state. The complexity of identifying $\Xi_c(2965)$ is revealed by the fact that our model predicts two states, which adapt equally well for this state. The first $\Xi_c(2965)$ assignment is $J^P = 3/2^-$ with $S = 3/2$; this belongs to the sextet, and refers to a P_λ-wave excitation. The experimental mass and the width are well reproduced. The identification of $\Xi_c(2965)$ as $J^P = 3/2^-$ is compatible with the QCD sum rule approach [24,76], but in Ref. [77] the $\Xi_c(2965)$ resonance may correspond to the λ-mode $\Xi_c'(1P)$ state with $J^P = 5/2^-$. A second identification of $\Xi_c(2965)$ is a P_ρ-wave $J^P = 1/2^-$ state with $S = 3/2$; thus, $\Xi_c(2965)$ would belong to the anti-3-plet, since we obtain a similar mass of 2978 ± 6 MeV and width that is compatible with the experimental value. It is noteworthy that, if the experiments confirm that there is a Ξ_c state at 2965 MeV which it is not a Roper state, it would mean that we could identify this state as a member of the sextet or anti-3-plet: either as a P_λ-wave excitation or as a P_ρ-wave excitation. The latter would imply that the charmed baryons behave as three-quark systems, instead of quark-diquark systems. Future experiments will help disentangle this puzzle. There is a similar situation for $\Xi_c(3055)$, where we also have two possible assignments. The first one is its identification as the first P_ρ-wave state in the sextet, with $J^P = 1/2^-$ and $S = 1/2$. Our theoretical mass exhibits a deviation of only 6 MeV, but the width is overestimated. The other possible $\Xi_c(3055)$ assignment is to the P_ρ-wave state in the anti-3-plet, with $J^P = 5/2^-$ and $S = 3/2$. Here, the mass is well reproduced and the width is overestimated. $\Xi_c(3080)$ is identified as the P_ρ-wave of the sextet, with $J^P = 1/2^-$ and $S = 3/2$. While our theoretical mass is well reproduced, our width is overestimated. Also, there are other possible interpretations of $\Xi_c(3055)$ and $\Xi_c(3080)$. For instance in Ref. [78] the authors identified $\Xi_c(3055)$ and $\Xi_c(3080)$ together from the D-wave charmed baryon doublet of the anti-3-plet. Finally, $\Xi_c(3123)$ is identified as the first D_λ-wave excitation $J^P = 3/2^+$ with $S = 1/2$ of the anti-3-plet. The mass is well reproduced in our model but the width is overestimated.

4. Λ_c

Our results for Λ_c baryons are reported in Table VIII. The Λ_c^+ is identified as the ground state $J^P = 1/2^+$, with $S = 1/2$; its mass is well reproduced, with a small deviation of 15 MeV. For the excited states, we can observe a systematic deviation that exhibits the failure of the h.o. potential for these states. Nevertheless, the patterns in the theoretical mass spectrum can describe the experimental one. $\Lambda_c(2595)^+$ and $\Lambda_c(2625)^+$ are identified as our two P_λ-wave excitations $J^P = 1/2^-$ and $J^P = 3/2^-$, respectively, both with $S = 1/2$; their masses are reproduced with a deviation of 15 MeV. The theoretical width is compatible with the experimental for $\Lambda_c(2595)^+$ states value but overestimated for $\Lambda_c(2625)^+$. The identification of $\Lambda_c(2595)^+$ and $\Lambda_c(2625)^+$ are in agreement with various quark models [16,18–20]. If the $\Lambda_c(2765)^+$ or $\Sigma_c(2765)$ state is identified as the Λ_c state in our model, there is no resonance within this energy region. Although it is close in energy to our predicted state $\Lambda_c(2800)^+$, $\Lambda_c(2765)^+$ is expected to be a Roper-like resonance. Consequently, we fail to reproduce the $\Lambda_c(2765)^+$ mass in our model, since our first theoretical radial excitation is the $\Lambda_c(3007)^+$ state. The observed $\Lambda_c(2860)^+$ is identified with a $J^P = 3/2^+$ state, having a significant predicted mass deviation of 100 MeV, but the theoretical decay width is well reproduced. Finally, the observed $\Lambda_c(2880)^+$ is identified with a $J^P = 5/2^+$ state. In this case, we also have a predicted mass with a deviation of 100 MeV, and a large deviation of the decay width. The identifications of $\Lambda_c(2860)^+$ and $\Lambda_c(2880)^+$ as D-wave states, $J^P = 3/2^+$ and $J^P = 5/2^+$ are in agreement with quark models [16,18–20].

V. COMPARISON BETWEEN THE THREE-QUARK AND QUARK-DIQUARK STRUCTURES

In the light baryon sector, the successful constituent quark model reproduces the baryon mass spectra by assuming that the constituent quarks have roughly the same mass. This implies that the two oscillators, ρ and λ, have the same frequency, $\omega_\rho \simeq \omega_\lambda$, meaning that the λ and ρ modes are degenerate in the mass spectrum. In the charm sector, we have a mass splitting between the λ and ρ modes, which is given by $\omega_\lambda - \omega_\rho \simeq 122$ MeV for Ω_c baryons, by $\omega_\lambda - \omega_\rho \simeq 147$ MeV for Ξ_c and Ξ_c' baryons, and by $\omega_\lambda - \omega_\rho \simeq 183$ MeV for Σ_c and Λ_c baryons. Consequently, we may expect to find the ρ−mode excited states in future experiments. However, given that the ρ states have not been observed yet, it seems that the charmed baryons can have a special internal structure which corresponds to the quark-diquark configuration. The reduction of the effective degrees of freedom in the quark-diquark picture means fewer predicted states. We notice that in the case of Λ_c and Ξ_c baryons, the number of states decreases drastically in the quark-diquark model, see Tables VIII and VII respectively. The lack of experimental data prevents us from reaching a decisive conclusion about which description is better.

For instance, for the Ω_c baryons, we have identified all the five P_λ-wave excited states with the experimental ones. We also expect to observe the two P_ρ-wave excited states, $\Omega_c(3129)$ with $J^P = 1/2^-$, and $\Omega_c(3156)$ with $J^P = 3/2^-$. The existence of these states may indicate that the charmed baryons are not quark-diquark systems.

VI. CONCLUSIONS

We have calculated the mass spectra, the strong partial decay widths and the total decay widths of the charmed baryons up to the D-wave. All charmed baryons are simultaneously described by a global fit in which the same set of model parameters predicts the charmed baryon masses and strong partial decay widths in all the possible decay channels up to the D-wave. Moreover, the charmed baryon mass spectra are given in both the three-quark and the quark-diquark schemes. Propagation of the parameter uncertainties via a Monte Carlo bootstrap method is also included. This is often missing in theoretical papers on this subject. Nevertheless, it is necessary in order to guarantee a rigorous treatment of the uncertainties in the predicted mass spectra and decay widths. Our mass and strong partial decay width predictions are in good agreement with the available experimental data, and show the ability to guide future experimental searches by LHCb, Belle and Belle II.

Moreover, for all the possible decay channels, we provide the flavor coupling coefficients, which are relevant to further theoretical investigations on charmed baryon strong decay widths. To the best of our knowledge, considering that the calculations of the strong decay widths are barely sensitive to the specific model used, our strong partial decay width predictions constitute the most complete calculation in the charmed baryon sector up to date.

ACKNOWLEDGMENTS

This work was supported in part by INFN, sezione di Genova. The authors acknowledge financial support from CONACyT, México (postdoctoral fellowship for H. G.-T.); National Research Foundation of Korea (grants No. 2020R1I1A1A01066423, No. 2019R1I1A3A01058933, No. 2018R1A6A1A06024970).

APPENDIX A: BARYON WAVE FUNCTIONS

1. The harmonic oscillator wave functions

In the heavy-light sector, the ρ- and λ-modes decouple; therefore, they can be distinguished through an analysis of the heavy-light baryon mass spectra. This is because there is a difference in frequency between the ρ- and λ-modes,

$$\omega_\rho = \sqrt{\frac{3K_Q}{m_\rho}} \quad \text{and} \quad \omega_\lambda = \sqrt{\frac{3K_Q}{m_\lambda}}, \tag{A1}$$

where m_ρ and m_λ are defined in Sec. II B. We write the baryon wave functions in terms of ω_ρ and ω_λ by using the relation $\alpha^2_{\rho,\lambda} = \omega_{\rho,\lambda} m_{\rho,\lambda}$.

Also, we use the standard Jacobi coordinates:

$$\begin{aligned} \mathbf{p}_\rho &= \frac{1}{2}(\mathbf{p_1} - \mathbf{p_2}), \\ \mathbf{p}_\lambda &= \frac{1}{3}(\mathbf{p_1} + \mathbf{p_2} - 2\mathbf{p_3}), \\ \mathbf{P_{cm}} &= \mathbf{p_1} + \mathbf{p_2} + \mathbf{p_3}, \end{aligned} \tag{A2}$$

for the baryon, and

$$\mathbf{q_c} = \frac{1}{2}(\mathbf{p_3} - \mathbf{p_5}), \tag{A3}$$

for the meson. In this coordinate system, $\mathbf{p_3}$ refers to the charm quark and $\mathbf{p_{1,2}}$ to the light quarks. Finally, $\mathbf{p_5}$ is the antiquark momentum.

For the S-wave charmed baryon, we have,

$$\psi(0,0,0,0) = 3^{3/4}\left(\frac{1}{\pi\omega_\rho m_\rho}\right)^{\frac{3}{4}}\left(\frac{1}{\pi\omega_\lambda m_\lambda}\right)^{\frac{3}{4}} \times \exp\left[-\frac{\mathbf{p}_\rho^2}{2\omega_\rho m_\rho} - \frac{\mathbf{p}_\lambda^2}{2\omega_\lambda m_\lambda}\right]. \tag{A4}$$

For the P-wave charmed baryon, we have,

$$\psi(1,m,0,0) = -i3^{3/4}\left(\frac{8}{3\sqrt{\pi}}\right)^{1/2}\left(\frac{1}{\omega_\rho m_\rho}\right)^{5/4}\mathcal{Y}_1^m(\mathbf{p}_\rho) \times \left(\frac{1}{\pi\omega_\lambda m_\lambda}\right)^{3/4}\exp\left[-\frac{\mathbf{p}_\rho^2}{2\omega_\rho m_\rho} - \frac{\mathbf{p}_\lambda^2}{2\omega_\lambda m_\lambda}\right], \tag{A5}$$

$$\psi(0,0,1,m) = -i3^{3/4}\left(\frac{8}{3\sqrt{\pi}}\right)^{1/2}\left(\frac{1}{\omega_\lambda m_\lambda}\right)^{5/4}\mathcal{Y}_1^m(\mathbf{p}_\lambda) \times \left(\frac{1}{\pi\omega_\rho m_\rho}\right)^{3/4}\exp\left[-\frac{\mathbf{p}_\rho^2}{2\omega_\rho m_\rho} - \frac{\mathbf{p}_\lambda^2}{2\omega_\lambda m_\lambda}\right]. \tag{A6}$$

For the D-wave charmed baryon, we have,

$$\psi(2,m,0,0) = 3^{3/4}\left(\frac{16}{15\sqrt{\pi}}\right)^{1/2}\left(\frac{1}{\omega_\rho m_\rho}\right)^{7/4}\mathcal{Y}_2^m(\mathbf{p}_\rho) \times \left(\frac{1}{\pi\omega_\lambda m_\lambda}\right)^{3/4}\exp\left[-\frac{\mathbf{p}_\rho^2}{2\omega_\rho m_\rho} - \frac{\mathbf{p}_\lambda^2}{2\omega_\lambda m_\lambda}\right], \tag{A7}$$

$$\psi(0,0,2,m) = 3^{3/4}\left(\frac{16}{15\sqrt{\pi}}\right)^{1/2}\left(\frac{1}{\omega_\lambda m_\lambda}\right)^{7/4}\mathcal{Y}_2^m(\mathbf{p}_\lambda) \times \left(\frac{1}{\pi\omega_\rho m_\rho}\right)^{3/4}\exp\left[-\frac{\mathbf{p}_\rho^2}{2\omega_\rho m_\rho} - \frac{\mathbf{p}_\lambda^2}{2\omega_\lambda m_\lambda}\right], \tag{A8}$$

$$\psi(1,m,1,m') = -3^{3/4}\left(\frac{8}{3\sqrt{\pi}}\right)^{1/2}\left(\frac{1}{\omega_\rho m_\rho}\right)^{5/4}\mathcal{Y}_1^m(\mathbf{p}_\rho) \times \left(\frac{8}{3\sqrt{\pi}}\right)^{1/2}\left(\frac{1}{\omega_\lambda m_\lambda}\right)^{5/4}\mathcal{Y}_1^{m'}(\mathbf{p}_\lambda) \times \exp\left[-\frac{\mathbf{p}_\rho^2}{2\omega_\rho m_\rho} - \frac{\mathbf{p}_\lambda^2}{2\omega_\lambda m_\lambda}\right]. \tag{A9}$$

Here $\mathcal{Y}_l^m(\mathbf{p})$ is the solid harmonic. The wave functions of the first radially excited charmed baryons $\psi(k_\lambda, k_\rho)$ are

$$\psi(1,0) = 3^{3/4}\left(\frac{2}{3}\right)^{1/2}\left(\frac{1}{\pi^4\omega_\lambda m_\lambda\omega_\rho m_\rho}\right)^{3/4}\left[\frac{3}{2}-\frac{\mathbf{p}_\lambda^2}{\omega_\lambda m_\lambda}\right] \times \exp\left[-\frac{\mathbf{p}_\rho^2}{2\omega_\rho m_\rho}-\frac{\mathbf{p}_\lambda^2}{2\omega_\lambda m_\lambda}\right], \quad \text{(A10)}$$

$$\psi(0,1) = 3^{3/4}\left(\frac{2}{3}\right)^{1/2}\left(\frac{1}{\pi^4\omega_\lambda m_\lambda\omega_\rho m_\rho}\right)^{3/4}\left[\frac{3}{2}-\frac{\mathbf{p}_\rho^2}{\omega_\rho m_\rho}\right] \times \exp\left[-\frac{\mathbf{p}_\rho^2}{2\omega_\rho m_\rho}-\frac{\mathbf{p}_\lambda^2}{2\omega_\lambda m_\lambda}\right]. \quad \text{(A11)}$$

The ground state wave function of the meson is

$$\psi(0,0) = \left(\frac{R^2}{\pi}\right)^{3/4}\exp\left[-\frac{R^2(\mathbf{p}_3-\mathbf{p}_5)^2}{8}\right]. \quad \text{(A12)}$$

APPENDIX B: CHARMED-BARYON FLAVOR WAVE FUNCTIONS

In the charm sector, we consider the **6-plet** and the **$\bar{3}$-plet** representation of the flavor wave functions. In the following subsections, we give the flavor wave functions of a charmed baryon A_c and its isospin quantum numbers $|A_c, I, M_I\rangle$.

1. 6-plet

$$|\Omega_c,0,0\rangle \coloneqq |ssc\rangle \quad \text{(B1)}$$

$$|\Xi_c'^0,1/2,-1/2\rangle \coloneqq \frac{1}{\sqrt{2}}(|dsc\rangle+|sdc\rangle) \quad \text{(B2)}$$

$$|\Xi_c'^+,1/2,1/2\rangle \coloneqq \frac{1}{\sqrt{2}}(|usc\rangle+|suc\rangle) \quad \text{(B3)}$$

$$|\Sigma_c^{++},1,1\rangle \coloneqq |uuc\rangle \quad \text{(B4)}$$

$$|\Sigma_c^0,1,-1\rangle \coloneqq |ddc\rangle \quad \text{(B5)}$$

$$|\Sigma_c^+,1,0\rangle \coloneqq \frac{1}{\sqrt{2}}(|udc\rangle+|duc\rangle) \quad \text{(B6)}$$

2. $\bar{3}$-plet

$$|\Xi_c^0,1/2,-1/2\rangle \coloneqq \frac{1}{\sqrt{2}}(|dsc\rangle-|sdc\rangle) \quad \text{(B7)}$$

$$|\Xi_c^+,1/2,1/2\rangle \coloneqq \frac{1}{\sqrt{2}}(|usc\rangle-|suc\rangle) \quad \text{(B8)}$$

$$|\Lambda_c^+,0,0\rangle \coloneqq \frac{1}{\sqrt{2}}(|udc\rangle-|duc\rangle) \quad \text{(B9)}$$

APPENDIX C: LIGHT-BARYON WAVE FUNCTIONS

Whenever our final states contained a light baryon, we used the following conventions, considering the S_3 invariant space-spin-flavor ($\Psi=\psi\chi\phi$). Thus, the light-baryon wave functions are given by

$$\begin{aligned}
&{}^2 8[56,L^P]: \psi_S(\chi_\rho\phi_\rho+\chi_\lambda\phi_\lambda)/\sqrt{2},\\
&{}^2 8[70,L^P]: [\psi_\rho(\chi_\rho\phi_\lambda+\chi_\lambda\phi_\rho)+\psi_\lambda(\chi_\rho\phi_\rho-\chi_\lambda\phi_\lambda)]/2,\\
&{}^4 8[70,L^P]: (\psi_\rho\phi_\rho+\psi_\lambda\phi_\lambda)\chi_S/\sqrt{2},\\
&{}^2 8[20,L^P]: \psi_A(\chi_\rho\phi_\lambda-\chi_\lambda\phi_\rho)/\sqrt{2},\\
&{}^4 10[56,L^P]: \psi_S\chi_S\phi_S,\\
&{}^2 10[70,L^P]: (\psi_\rho\chi_\rho+\psi_\lambda\chi_\lambda)\phi_S/\sqrt{2},\\
&{}^2 1[70,L^P]: (\psi_\rho\chi_\lambda-\psi_\lambda\chi_\rho)\phi_A/\sqrt{2},\\
&{}^4 1[20,L^P]: \psi_A\chi_S\phi_A. \qquad \text{(C1)}
\end{aligned}$$

The quark orbital angular momentum $\mathbf{L}$ is coupled with the spin $\mathbf{S}$ to yield the total angular momentum $\mathbf{J}$ of the baryon.

1. Light-baryon flavor wave functions

For the flavor wave functions $|(p,q),I,M_I,Y\rangle$ we adopt the convention of Ref. [79] with $(p,q)=(g_1-g_2,g_2)$.

(i) The octet baryons

$$\begin{aligned}
\left|(1,1),\frac{1}{2},\frac{1}{2},1\right\rangle &: \phi_\rho(p)=\frac{1}{\sqrt{2}}[|udu\rangle-|duu\rangle]\\
&: \phi_\lambda(p)=\frac{1}{\sqrt{6}}[2|uud\rangle-|udu\rangle - |duu\rangle] \qquad \text{(C2)}
\end{aligned}$$

$$\begin{aligned}
|(1,1),1,1,0\rangle &: \phi_\rho(\Sigma^+)=\frac{1}{\sqrt{2}}[|suu\rangle-|usu\rangle]\\
&: \phi_\lambda(\Sigma^+)=\frac{1}{\sqrt{6}}[|suu\rangle+|usu\rangle - 2|uus\rangle] \qquad \text{(C3)}
\end{aligned}$$

$$\begin{aligned}
|(1,1),0,0,0\rangle &: \phi_\rho(\Lambda)=\frac{1}{\sqrt{12}}[2|uds\rangle-2|dus\rangle - |dsu\rangle+|sdu\rangle - |sud\rangle+|usd\rangle]\\
&: \phi_\lambda(\Lambda)=\frac{1}{2}[-|dsu\rangle-|sdu\rangle + |sud\rangle+|usd\rangle] \qquad \text{(C4)}
\end{aligned}$$

$$\left|(1,1),\frac{1}{2},\frac{1}{2},-1\right\rangle : \phi_\rho(\Xi^0) = \frac{1}{\sqrt{2}}[|sus\rangle - |uss\rangle]$$
$$: \phi_\lambda(\Xi^0) = \frac{1}{\sqrt{6}}[2|ssu\rangle - |sus\rangle - |uss\rangle] \quad (C5)$$

(ii) The decuplet baryons

$$\left|(3,0),\frac{3}{2},\frac{3}{2},1\right\rangle : \phi_S(\Delta^{++}) = |uuu\rangle \quad (C6)$$

$$|(3,0),1,1,0\rangle : \phi_S(\Sigma^+) = \frac{1}{\sqrt{3}}[|suu\rangle + |usu\rangle + |uus\rangle] \quad (C7)$$

$$\left|(3,0),\frac{1}{2},\frac{1}{2},-1\right\rangle : \phi_S(\Xi^0) = \frac{1}{\sqrt{3}}[|ssu\rangle + |sus\rangle + |uss\rangle] \quad (C8)$$

$$|(3,0),0,0,-2\rangle : \phi_S(\Omega^-) = |sss\rangle \quad (C9)$$

(iii) The singlet baryon

$$|(0,0),0,0,0\rangle : \phi_A(\Lambda) = \frac{1}{\sqrt{6}}[|uds\rangle - |dus\rangle + |dsu\rangle - |sdu\rangle + |sud\rangle - |usd\rangle] \quad (C10)$$

APPENDIX D: MESON FLAVOR WAVE FUNCTIONS

In the following subsections, we give the flavor wave functions of a C meson and its isospin quantum numbers $|C, I, M_I\rangle$.

1. Pseudoscalar mesons

Since the mixing angle $\theta_{\eta\eta'}$ between η and η' is small, we set $\theta_{\eta\eta'} = 0$. Thus, we identify $\eta = \eta_8$ and $\eta' = \eta_1$.

(i) The octet meson

$$|\pi^+,1,1\rangle = -|u\bar{d}\rangle$$
$$|\pi^0,1,0\rangle = \frac{1}{\sqrt{2}}[|u\bar{u}\rangle - |d\bar{d}\rangle]$$
$$|\pi^-,1,-1\rangle = |d\bar{u}\rangle$$
$$|K^+,1/2,1/2\rangle = -|u\bar{s}\rangle$$
$$|K^-,1/2,-1/2\rangle = |s\bar{u}\rangle$$
$$|K^0,1/2,-1/2\rangle = -|d\bar{s}\rangle$$
$$|\bar{K}^0,1/2,1/2\rangle = -|s\bar{d}\rangle$$
$$|\eta,0,0\rangle = \frac{1}{\sqrt{6}}[|u\bar{u}\rangle + |d\bar{d}\rangle - 2|s\bar{s}\rangle] \quad (D1)$$

(ii) The singlet meson

$$|\eta',0,0\rangle = \frac{1}{\sqrt{3}}[|u\bar{u}\rangle + |d\bar{d}\rangle + |s\bar{s}\rangle] \quad (D2)$$

2. Vector mesons

We consider that the ϕ meson is a pure $s\bar{s}$ state; thus, we have the following wave functions:

(i) The octet mesons

$$|\rho^+,1,1\rangle = -|u\bar{d}\rangle$$
$$|\rho^0,1,0\rangle = \frac{1}{\sqrt{2}}[|u\bar{u}\rangle - |d\bar{d}\rangle]$$
$$|\rho^-,1,-1\rangle = |d\bar{u}\rangle$$
$$|K^{*+},1/2,1/2\rangle = -|u\bar{s}\rangle$$
$$|K^{*-},1/2,-1/2\rangle = |s\bar{u}\rangle$$
$$|K^{*0},1/2,-1/2\rangle = -|d\bar{s}\rangle$$
$$|\bar{K}^{*0},1/2,1/2\rangle = -|s\bar{d}\rangle$$
$$|\omega,0,0\rangle = \frac{1}{\sqrt{2}}[|u\bar{u}\rangle + |d\bar{d}\rangle] \quad (D3)$$

(ii) The singlet meson

$$|\phi,0,0\rangle = |s\bar{s}\rangle \quad (D4)$$

3. Charmed mesons

In the case of charmed-D mesons, the flavor wave functions are the same for the pseudoscalar and vector states. We use the following flavor wave functions:

$$|D_s^{+*},0,0\rangle = |D_s^+,0,0\rangle = |c\bar{s}\rangle$$
$$|D^{+*},1/2,1/2\rangle = |D^+,1/2,1/2\rangle = |c\bar{d}\rangle$$
$$|D^{0*},1/2,-1/2\rangle = |D^0,1/2,-1/2\rangle = |c\bar{u}\rangle \quad (D5)$$

APPENDIX E: FLAVOR COUPLING

In the following subsections, we give the flavor coefficients $\mathcal{F}_{A\to BC}$ used to calculate the transition amplitudes. We compute $\mathcal{F}_{A\to BC} = \langle \phi_B\phi_C|\phi_0\phi_A\rangle$ where $\phi_{(A,B,C)}$ refers to the initial flavor wave function of a charmed baryon ϕ_{A_c}, final baryon ϕ_B, and final meson ϕ_C, respectively; $\phi_0^{45} = (u\bar{u} + d\bar{d} + s\bar{s})/\sqrt{3}$ is the flavor singlet-wave function of $SU(3)$. In addition, we compute the flavor decay coefficients of the isospin channels, since we assume that the isospin symmetry holds even though it is slightly broken. The corresponding charge channels are obtained by multiplying our $\mathcal{F}_{A\to BC}$ by the corresponding Clebsch-Gordan coefficient in the isospin space, using the convention of the isospin quantum numbers of the baryon and meson flavor wave functions found in Appendices B, C 1, and D. Thus, the flavor charge channel for a specific projection (I, M_I) in the isospin space is obtained as follows:

$$\begin{aligned}&\mathcal{F}_{A(I_A,M_{I_A})\to B(I_B,M_{I_B})C(I_C,M_{I_C})}\\&=\langle\phi_B,I_B,M_{I_B},\phi_C,I_C,M_{I_C}|\phi_0,0,0,\phi_A,I_A,M_{I_A}\rangle_F\\&=\langle I_B,M_{I_B},I_C,M_{I_C}|I_A,M_{I_A}\rangle\mathcal{F}_{A\to BC},\end{aligned}\tag{E1}$$

where $\langle I_B,M_{I_B},I_C,M_{I_C}|I_A,M_{I_A}\rangle$ is a Clebsch-Gordan coefficient and the flavor functions ϕ_i of each baryon and meson have a specific isospin projection M_I.

1. Charmed baryons and pseudoscalar mesons

We give the squared flavor-coupling coefficients, $\mathcal{F}^2_{A\to BC}$, when the final states have a pseudoscalar light meson. Here, A and B are charmed baryons, and the subindexes $\mathbf{6}_\mathrm{f}$ and $\bar{\mathbf{3}}_\mathrm{f}$ refer to the sextet and the antitriplet baryon multiplets. The C is a pseudoscalar meson and the subindexes $\mathbf{8}$ and $\mathbf{1}$ refer to the octet and singlet meson multiplets, respectively.

(i) $A_{\mathbf{6}_\mathrm{f}}\to B_{\mathbf{6}_\mathrm{f}}+C_{\mathbf{8}}$

$$\begin{pmatrix}\Omega_c\\\Sigma_c\\\Xi'_c\end{pmatrix}\to\begin{pmatrix}&\Xi'_cK&\Omega_c\eta\\\Xi'_cK&\Sigma_c\pi&\Sigma_c\eta\\\Sigma_cK&\Xi'_c\pi&\Xi'_c\eta\end{pmatrix}=\begin{pmatrix}&\frac{1}{3}&\frac{2}{9}\\\frac{1}{6}&\frac{1}{3}&\frac{1}{18}\\\frac{1}{4}&\frac{1}{8}&\frac{1}{72}\end{pmatrix}\tag{E2}$$

(ii) $A_{\mathbf{6}_\mathrm{f}}\to B_{\mathbf{6}_\mathrm{f}}+C_{\mathbf{1}}$

$$\begin{pmatrix}\Omega_c\\\Sigma_c\\\Xi'_c\end{pmatrix}\to\begin{pmatrix}\Omega_c\eta'\\\Sigma_c\eta'\\\Xi'_c\eta'\end{pmatrix}=\begin{pmatrix}\frac{1}{3}\\\frac{1}{9}\\\frac{1}{9}\end{pmatrix}\tag{E3}$$

(iii) $A_{\mathbf{6}_\mathrm{f}}\to B_{\bar{\mathbf{3}}_\mathrm{f}}+C_{\mathbf{8}}$

$$\begin{pmatrix}\Omega_c\\\Sigma_c\\\Xi'_c\end{pmatrix}\to\begin{pmatrix}&\Xi_cK&\\\Xi_cK&\Lambda_c\pi&\\\Lambda_cK&\Xi_c\pi&\Xi_c\eta\end{pmatrix}=\begin{pmatrix}&\frac{1}{3}&\\\frac{1}{6}&\frac{1}{2}&\\\frac{1}{12}&\frac{1}{8}&\frac{1}{72}\end{pmatrix}\tag{E4}$$

(iv) $A_{\mathbf{6}_\mathrm{f}}\to B_{\bar{\mathbf{3}}_\mathrm{f}}+C_{\mathbf{1}}$

$$(\Xi'_c)\to(\Xi_c\eta')=\begin{pmatrix}\frac{1}{9}\end{pmatrix}\tag{E5}$$

(v) $A_{\bar{\mathbf{3}}_\mathrm{f}}\to B_{\mathbf{6}_\mathrm{f}}+C_{\mathbf{8}}$

$$\begin{pmatrix}\Lambda_c\\\Xi_c\end{pmatrix}\to\begin{pmatrix}\Xi'_cK&\Sigma_c\pi&\\\Sigma_cK&\Xi'_c\pi&\Xi'_c\eta\end{pmatrix}=\begin{pmatrix}\frac{1}{6}&\frac{1}{2}&\\\frac{1}{4}&\frac{1}{8}&\frac{1}{72}\end{pmatrix}\tag{E6}$$

(vi) $A_{\bar{\mathbf{3}}_\mathrm{f}}\to B_{\mathbf{6}_\mathrm{f}}+C_{\mathbf{1}}$

$$(\Xi_c)\to(\Xi'_c\eta')=\begin{pmatrix}\frac{1}{9}\end{pmatrix}\tag{E7}$$

(vii) $A_{\bar{\mathbf{3}}_\mathrm{f}}\to B_{\bar{\mathbf{3}}_\mathrm{f}}+C_{\mathbf{8}}$

$$\begin{pmatrix}\Lambda_c\\\Xi_c\end{pmatrix}\to\begin{pmatrix}\Xi_cK&\Lambda_c\eta&\\\Lambda_cK&\Xi_c\pi&\Xi_c\eta\end{pmatrix}=\begin{pmatrix}\frac{1}{6}&\frac{1}{18}&\\\frac{1}{12}&\frac{1}{8}&\frac{1}{72}\end{pmatrix}\tag{E8}$$

(viii) $A_{\bar{\mathbf{3}}_\mathrm{f}}\to B_{\bar{\mathbf{3}}_\mathrm{f}}+C_{\mathbf{1}}$

$$\begin{pmatrix}\Lambda_c\\\Xi_c\end{pmatrix}\to\begin{pmatrix}\Lambda_c\eta'\\\Xi_c\eta'\end{pmatrix}=\begin{pmatrix}\frac{1}{9}\\\frac{1}{9}\end{pmatrix}\tag{E9}$$

2. Charmed baryons and vector mesons

We give the squared flavor-coupling coefficients, $\mathcal{F}^2_{A\to BC}$, when the final states have a vector-light meson. Here A and B are charmed baryons, and the subindexes $\mathbf{6}_\mathrm{f}$ and $\bar{\mathbf{3}}_\mathrm{f}$ refer to the sextet and the antitriplet baryon multiplets. The C is a vector meson and the subindexes $\mathbf{8}$ and $\mathbf{1}$ refer to the octet and singlet meson multiplets, respectively.

(i) $A_{\mathbf{6}_\mathrm{f}}\to B_{\mathbf{6}_\mathrm{f}}+C_{\mathbf{8}}$

$$\begin{pmatrix}\Omega_c\\\Sigma_c\\\Xi'_c\end{pmatrix}\to\begin{pmatrix}&\Xi'_cK^*&\\\Xi'_cK^*&\Sigma_c\rho&\Sigma_c\omega\\\Sigma_cK^*&\Xi'_c\rho&\Xi'_c\omega\end{pmatrix}=\begin{pmatrix}&\frac{1}{3}&\\\frac{1}{6}&\frac{1}{3}&\frac{1}{6}\\\frac{1}{4}&\frac{1}{8}&\frac{1}{24}\end{pmatrix}\tag{E10}$$

(ii) $A_{\mathbf{6}_\mathrm{f}}\to B_{\mathbf{6}_\mathrm{f}}+C_{\mathbf{1}}$

$$\begin{pmatrix}\Omega_c\\\Sigma_c\\\Xi'_c\end{pmatrix}\to\begin{pmatrix}\Omega_c\phi\\\Sigma_c\phi\\\Xi'_c\phi\end{pmatrix}=\begin{pmatrix}\frac{1}{9}\\0\\\frac{1}{2}\end{pmatrix}\tag{E11}$$

(iii) $A_{\mathbf{6}_{\rm f}} \to B_{\bar{\mathbf{3}}_{\rm f}} + C_{\mathbf{8}}$

$$\begin{pmatrix} \Omega_c \\ \Sigma_c \\ \Xi'_c \end{pmatrix} \to \begin{pmatrix} & \Xi_c K^* & \\ \Xi_c K^* & \Lambda_c \rho & \\ \Lambda_c K^* & \Xi_c \rho & \Xi_c \omega \end{pmatrix} = \begin{pmatrix} & \frac{1}{3} & \\ \frac{1}{6} & \frac{1}{3} & \\ \frac{1}{12} & \frac{1}{8} & \frac{1}{24} \end{pmatrix} \quad \text{(E12)}$$

(iv) $A_{\mathbf{6}_{\rm f}} \to B_{\bar{\mathbf{3}}_{\rm f}} + C_{\mathbf{1}}$

$$(\Xi'_c) \to (\Xi_c \phi) = \left(\frac{1}{12}\right) \quad \text{(E13)}$$

(v) $A_{\bar{\mathbf{3}}_{\rm f}} \to B_{\mathbf{6}_{\rm f}} + C_{\mathbf{8}}$

$$\begin{pmatrix} \Lambda_c \\ \Xi_c \end{pmatrix} \to \begin{pmatrix} \Xi'_c K^* & \Sigma_c \rho & \\ \Sigma_c K^* & \Xi'_c \rho & \Xi'_c \omega \end{pmatrix} = \begin{pmatrix} \frac{1}{6} & \frac{1}{2} & \\ \frac{1}{4} & \frac{1}{8} & \frac{1}{24} \end{pmatrix} \quad \text{(E14)}$$

(vi) $A_{\bar{\mathbf{3}}_{\rm f}} \to B_{\mathbf{6}_{\rm f}} + C_{\mathbf{1}}$

$$(\Xi_c) \to (\Xi'_c \phi) = \left(\frac{1}{12}\right) \quad \text{(E15)}$$

(vii) $A_{\bar{\mathbf{3}}_{\rm f}} \to B_{\bar{\mathbf{3}}_{\rm f}} + C_{\mathbf{8}}$

$$\begin{pmatrix} \Lambda_c \\ \Xi_c \end{pmatrix} \to \begin{pmatrix} \Xi_c K^* & \Lambda_c \omega & \\ \Lambda_c K^* & \Xi_c \rho & \Xi_c \omega \end{pmatrix} = \begin{pmatrix} \frac{1}{6} & \frac{1}{6} & \\ \frac{1}{12} & \frac{1}{8} & \frac{1}{24} \end{pmatrix} \quad \text{(E16)}$$

(viii) $A_{\bar{\mathbf{3}}_{\rm f}} \to B_{\bar{\mathbf{3}}_{\rm f}} + C_{\mathbf{1}}$

$$\begin{pmatrix} \Lambda_c \\ \Xi_c \end{pmatrix} \to \begin{pmatrix} \Lambda_c \phi \\ \Xi_c \phi \end{pmatrix} = \begin{pmatrix} 0 \\ \frac{1}{12} \end{pmatrix} \quad \text{(E17)}$$

3. Light baryons and charm-(pseudoscalar/vector) mesons

We give the $\mathcal{F}^2_{A\to BC}$ when the final states have a light baryon and a charm-(pseudoscalar/vector) meson. Since the mesons D^0 and D^+ form an isospin doublet, both are treated as D in the tables; whereas D_s is separated by the strangeness content. The subindexes $\mathbf{6}_{\rm f}$ and $\bar{\mathbf{3}}_{\rm f}$ refer to the sextet and the antitriplet baryon multiplets for the initial charmed baryon A, whereas the final B baryons can have subindexes **8** or **10**, according to whether the final light baryon belongs to the octet or decuplet baryon multiplets. Additionally, owing to the symmetry of the wave functions of the octet-light baryons, see Appendix C 1, we can have only ρ or λ contributions in the final states, as indicated by a superindex.

(i) $A_{\mathbf{6}_{\rm f}} \to B_{\mathbf{10}} + C$

$$\begin{pmatrix} \Omega_c \\ \Sigma_c \\ \Xi'_c \end{pmatrix} \to \begin{pmatrix} \Xi^*_{10} D & \Omega_{10} D_s \\ \Delta D & \Sigma^*_{10} D_s \\ \Sigma^*_{10} D & \Xi^*_{10} D_s \end{pmatrix} = \begin{pmatrix} \frac{2}{9} & \frac{1}{3} \\ \frac{4}{9} & \frac{1}{9} \\ \frac{1}{3} & \frac{2}{9} \end{pmatrix} \quad \text{(E18)}$$

(ii) $A_{\mathbf{6}_{\rm f}} \to B_{\mathbf{8}} + C$

$$\begin{pmatrix} \Omega_c \\ \Sigma_c \\ \Xi'_c \end{pmatrix} \to \begin{pmatrix} & \Xi^\lambda_8 D \\ N^\lambda D & \Sigma^\lambda_8 D_s \\ \Sigma^\lambda_8 D & \Xi^\lambda_8 D_s \end{pmatrix} = \begin{pmatrix} & \frac{4}{9} \\ \frac{2}{9} & \frac{2}{9} \\ \frac{1}{6} & \frac{1}{9} \end{pmatrix} \quad \text{(E19)}$$

(iii) $A_{\bar{\mathbf{3}}_{\rm f}} \to B_{\mathbf{8}} + C$

$$\begin{pmatrix} \Lambda_c \\ \Xi_c \end{pmatrix} \to \begin{pmatrix} N^\rho D & \Lambda^\rho_8 D_s & \\ \Sigma^\rho_8 D & \Xi^\rho_8 D_s & \Lambda^\rho_8 D \end{pmatrix} = \begin{pmatrix} \frac{2}{3} & \frac{2}{9} & \\ \frac{1}{2} & \frac{1}{3} & \frac{1}{18} \end{pmatrix} \quad \text{(E20)}$$

APPENDIX F: PARTIAL DECAY WIDTHS

The partial decay widths, $\Gamma_{A\to BC}$, of an initial baryon A decaying to a final baryon B plus a meson C, in all the open-flavor channels, are shown in Tables IX–XIII. Here, we give the contribution of the isospin channels. The charge channel width for the A baryon with isospin projection $|A, I, M_{I_A}\rangle$ can be obtained as follows

$$\Gamma_{A(I_A,M_{I_A})\to B(I_B,M_{I_B})C(I_C,M_{I_C})} = \langle I_B, M_{I_B}, I_C, M_{I_C} | I_A, M_{I_A}\rangle^2 \Gamma_{A\to BC}, \quad \text{(F1)}$$

where $\langle I_B, M_{I_B}, I_C, M_{I_C} | I_A, M_{I_A}\rangle$ is a Clebsch-Gordan coefficient, and the partial decay width $\Gamma_{A\to BC}$ can be extracted from Tables IX–XIII.

TABLE IX. $\Omega_c(ssc)$ state partial decay widths (in MeV). The order of the states is the same as in Table IV. The predicted masses, reported in Table IV, are obtained by the three-quark model Hamiltonian of Eqs. (1) and (2). The partial decay widths are computed by means of Eq. (7). For each state is also reported the spectroscopic notation ${}^{2S+1}L_J$, where $\mathbf{J} = \mathbf{L}_{\rm tot} + \mathbf{S}_{\rm tot}$ is the total angular momentum, $\mathbf{S}_{\rm tot} = \mathbf{S}_\rho + \frac{1}{2}$, and $\mathbf{L}_{\rm tot} = \mathbf{l}_\rho + \mathbf{l}_\lambda$. The partial decay widths denoted by 0 and – are forbidden by phase space and selection rules, respectively.

$\Omega_c(ssc)$ $\mathcal{F} = \mathbf{6}_{\rm f}$	$\Xi_c K$	$\Xi'_c K$	$\Xi^*_c K$	$\Xi_c K^*$	$\Xi'_c K^*$	$\Xi^*_c K^*$	$\Omega_c \eta$	$\Omega^*_c \eta$	$\Omega_c \phi$	$\Omega^*_c \phi$	$\Omega_c \eta'$	$\Omega^*_c \eta'$	$\Xi_8 D$	$\Xi_{10} D$	Predicted $\Gamma_{\rm tot}$
$\Omega_c(2709)^2S_{1/2}$	0	0	0	0	0	0	0	0	0	0	0	0	0	0	0
$\Omega_c(2778)^4S_{3/2}$	0	0	0	0	0	0	0	0	0	0	0	0	0	0	0
$\Omega_c(3008)^2P_{1/2}$	4.1	0	0	0	0	0	0	0	0	0	0	0	0	0	4.1
$\Omega_c(3050)^4P_{1/2}$	7.5	0.1	0	0	0	0	0	0	0	0	0	0	0	0	7.6
$\Omega_c(3035)^2P_{3/2}$	26.3	0	0	0	0	0	0	0	0	0	0	0	0	0	26.3
$\Omega_c(3077)^4P_{3/2}$	6.3	0.4	0	0	0	0	0	0	0	0	0	0	0	0	6.7
$\Omega_c(3122)^4P_{5/2}$	40.9	8.9	0.3	0	0	0	0	0	0	0	0	0	0	0	50.1
$\Omega_c(3129)^2P_{1/2}$	—	8.9	5.5	0	0	0	0	0	0	0	0	0	0	0	14.4
$\Omega_c(3156)^2P_{3/2}$	—	61.1	10.5	0	0	0	0	0	0	0	0	0	0	0	71.6
$\Omega_c(3315)^2D_{3/2}$	1.9	1.8	2.3	0	0	0	0.3	—	0	0	0	0	4.3	0	10.6
$\Omega_c(3360)^2D_{5/2}$	5.4	5.1	0.5	0	0	0	1.2	—	0	0	0	0	12.2	0	24.4
$\Omega_c(3330)^4D_{1/2}$	0.2	0.2	3.3	0	0	0	0.1	0.1	0	0	0	0	12.3	0	16.2
$\Omega_c(3357)^4D_{3/2}$	2.0	0.5	5.2	0.2	0	0	0.2	0.6	0	0	0	0	21.7	0	30.4
$\Omega_c(3402)^4D_{5/2}$	5.0	1.2	5.0	1.6	0	0	0.3	1.2	0	0	0	0	46.9	1.1	62.3
$\Omega_c(3466)^4D_{7/2}$	7.8	2.0	5.0	2.6	0	0	0.8	0.9	0	0	0	0	83.2	20.9	123.2
$\Omega_c(3342)^2S_{1/2}$	0.2	0.3	0.1	0	0	0	0.1	—	0	0	0	0	0.5	0	1.2
$\Omega_c(3411)^4S_{3/2}$	0.2	0.1	0.4	0.2	0	0	—	0.1	0	0	0	0	2.1	0.2	3.3
$\Omega_c(3585)^2S_{1/2}$	0.3	1.0	0.7	3.0	11.6	0.1	1.1	0.5	0	0	0	0	—	—	18.3
$\Omega_c(3654)^4S_{3/2}$	0.1	0.1	1.2	2.8	1.0	17.2	0.2	1.4	0	0	—	0	—	—	24.0
$\Omega_c(3437)^2D_{3/2}$	—	6.5	107.0	53.5	0	0	4.0	27.0	0	0	0	0	—	—	198.0
$\Omega_c(3482)^2D_{5/2}$	—	56.4	16.8	17.2	0.4	0	20.9	3.3	0	0	0	0	—	—	115.0
$\Omega_c(3446)^2P_{1/2}$	—	—	1.4	0.4	0	0	—	0.3	0	0	0	0	—	—	2.1
$\Omega_c(3473)^2P_{3/2}$	—	1.1	0.8	0.7	0	0	0.3	0.2	0	0	0	0	—	—	3.1
$\Omega_c(3464)^2S_{1/2}$	—	7.6	22.3	36.1	0.2	0	8.6	13.5	0	0	0	0	—	—	88.3
$\Omega_c(3558)^2D_{3/2}$	18.4	16.8	18.8	28.7	115.1	—	8.0	11.2	0	0	0	0	—	—	217.0
$\Omega_c(3603)^2D_{5/2}$	48.3	49.7	14.5	3.6	30.8	0.7	23.3	3.4	0	0	0	0	—	—	174.3
$\Omega_c(3573)^4D_{1/2}$	9.4	0.4	33.1	38.8	7.0	111.6	0.3	17.0	0	0	0	0	—	—	217.6
$\Omega_c(3600)^4D_{3/2}$	22.1	4.9	28.2	77.3	16.8	111.4	2.2	21.9	0	0	0	0	—	—	284.8
$\Omega_c(3645)^4D_{5/2}$	38.6	10.8	32.8	47.8	13.2	43.7	5.4	19.7	0	0	0	0	—	—	212.0
$\Omega_c(3708)^4D_{7/2}$	72.1	18.0	88.1	107.8	18.0	38.9	8.4	29.2	0.1	0	2.3	0.1	—	—	383.0

TABLE X. Same as IX, but for $\Sigma_c(nnc)$ states. The order of the states is the same as in Table V. The predicted masses, reported in Table V, are obtained by the three-quark model Hamiltonian of Eqs. (1) and (2). N_1^*, N_2^*, N_3^*, and N_4^* represent $N(1520)$, $N(1535)$, $N(1680)$, and $N(1720)$, respectively.

$\Sigma_c(nnc)$ $\mathcal{F}=\mathbf{6}_f$	$\Sigma_c\pi$	$\Sigma_c^*\pi$	$\Lambda_c\pi$	$\Sigma_c\eta$	Ξ_cK	$\Sigma_c\rho$	$\Sigma_c^*\rho$	$\Lambda_c\rho$	$\Sigma_c^*\eta$	$\Sigma_c\eta'$	$\Sigma_c^*\eta'$	$\Xi_c'K$	Ξ_c^*K	Ξ_cK^*	$\Xi_c'K^*$	$\Xi_c^*K^*$	$\Sigma_c\omega$	$\Sigma_c^*\omega$	ND	Σ_8D_s	ND^*	ΔD	N_1^*D	N_2^*D	N_3^*D	N_4^*D	Predicted $\Gamma_{\rm tot}$
$\Sigma_c(2456)^2S_{1/2}$	0	0	1.7	0	0	0	0	0	0	0	0	0	0	0	0	0	0	0	0	0	0	0	0	0	0	0	1.7
$\Sigma_c(2525)^4S_{3/2}$	0	0	14.9	0	0	0	0	0	0	0	0	0	0	0	0	0	0	0	0	0	0	0	0	0	0	0	14.9
$\Sigma_c(2811)^2P_{1/2}$	2.2	17.4	0.1	0	0	0	0	0	0	0	0	0	0	0	0	0	0	0	0.8	0	0	0	0	0	0	0	20.5
$\Sigma_c(2853)^4P_{1/2}$	0.7	9.9	1.7	0	0	0	0	0	0	0	0	0	0	0	0	0	0	0	13.3	0	0	0	0	0	0	0	25.6
$\Sigma_c(2838)^2P_{3/2}$	28.7	2.8	45.2	0	0	0	0	0	0	0	0	0	0	0	0	0	0	0	9.0	0	0	0	0	0	0	0	85.7
$\Sigma_c(2880)^4P_{3/2}$	1.6	39.0	9.8	0	0	0	0	0	0	0	0	0	0	0	0	0	0	0	9.8	0	0	0	0	0	0	0	60.2
$\Sigma_c(2925)^4P_{5/2}$	10.5	22.8	64.8	0	0	0	0	0	0	0	0	0	0	0	0	0	0	0	65.4	0	0	0	0	0	0	0	163.5
$\Sigma_c(2994)^2P_{1/2}$	0.5	123.8	—	0.3	—	0	0	0	0	0	0	0	0	0	0	0	0	0	—	0	—	0	0	0	0	0	124.6
$\Sigma_c(3021)^2P_{3/2}$	64.0	55.4	—	5.4	—	0	0	0.2	0	0	0	0	0	0	0	0	0	0	—	0	—	0	0	0	0	0	125.0
$\Sigma_c(3175)^2D_{3/2}$	2.5	3.3	4.9	0.3	0.7	0	0	4.3	0.3	0	0	0.4	0.2	0	0	0	0	0	3.8	1.4	30.0	77.0	0	0	0	0	129.1
$\Sigma_c(3220)^2D_{5/2}$	7.6	1.8	12.8	0.8	1.9	0.1	0	0.3	0.1	0	0	1.3	0.1	0	0	0	0	0	11.3	4.5	77.4	96.1	0	0	0	0	216.1
$\Sigma_c(3190)^4D_{1/2}$	—	5.4	2.4	—	0.3	0	0	5.5	0.4	0	0	0.1	0.4	0	0	0	0	0	0.4	5.1	42.8	36.3	0	0	0	0	99.1
$\Sigma_c(3217)^4D_{3/2}$	0.7	5.4	5.8	0.1	0.8	0.1	0	12.2	0.8	0	0	0.2	0.9	0	0	0	0	0	17.1	8.4	46.1	56.9	0	0	0	0	155.5
$\Sigma_c(3262)^4D_{5/2}$	1.7	5.4	10.3	0.2	1.8	0.5	0	8.6	0.8	0	0	0.3	1.4	0	0	0	0.2	0	40.5	18.3	49.0	87.5	0	0	0	0	227.4
$\Sigma_c(3326)^4D_{7/2}$	2.7	12.2	19.0	0.3	3.0	0.8	0.3	13.7	0.8	0	0	0.7	1.0	0	0	0	0.4	0.1	64.1	35.0	77.4	153.1	0	0	0	0	385.1
$\Sigma_c(3202)^2S_{1/2}$	0.2	0.1	—	—	0.1	0	0	0.4	—	0	0	0.1	—	0	0	0	0	0	0.1	0.2	1.8	4.8	0	0	0	0	7.8
$\Sigma_c(3271)^4S_{3/2}$	—	0.2	—	—	0.1	—	0	0.5	0.1	0	0	—	0.1	0	0	0	—	0	0.1	0.8	1.0	3.9	0	0	0	0	6.7
$\Sigma_c(3567)^2S_{1/2}$	0.3	0.1	1.7	—	—	6.6	0.1	0.1	—	0.5	0.2	0.2	0.2	1.0	4.0	—	3.5	0.1	—	—	—	—	—	—	—	0	18.6
$\Sigma_c(3637)^4S_{3/2}$	0.2	0.4	2.6	—	—	0.2	9.2	0.2	—	0.1	0.6	—	0.2	0.8	0.3	6.0	0.1	4.8	—	—	—	—	—	—	—	—	25.7
$\Sigma_c(3358)^2D_{3/2}$	7.7	94.8	—	0.9	—	37.7	0.4	166.5	17.1	0	0	3.0	36.8	1.6	0	0	18.0	0.2	—	—	—	—	1.7	0.1	0	0	386.5
$\Sigma_c(3403)^2D_{5/2}$	77.0	78.6	—	9.3	—	3.8	6.1	84.8	4.2	0.3	0	20.6	5.5	2.4	0	0	1.9	2.9	—	—	—	—	20.6	15.6	0	0	333.6
$\Sigma_c(3367)^2P_{1/2}$	—	1.7	—	—	—	0.2	—	1.6	0.2	0	0	—	0.3	—	0	0	0.1	—	—	—	—	—	3.2	0.7	0	0	8.0
$\Sigma_c(3394)^2P_{3/2}$	1.0	0.9	—	0.1	—	0.1	—	1.7	0.1	0	0	0.3	0.2	—	0	0	—	—	—	—	—	—	24.3	3.5	0	0	32.2
$\Sigma_c(3385)^2S_{1/2}$	8.6	4.4	—	0.4	—	23.7	4.9	7.5	1.9	0	0	3.5	9.4	3.7	0	0	11.9	2.3	—	—	—	—	16.7	0.9	0	0	99.8
$\Sigma_c(3540)^2D_{3/2}$	43.6	4.5	84.1	4.2	9.9	159.7	0.4	3.1	2.0	3.3	2.9	8.4	7.7	12.4	46.8	0	81.8	0.2	—	—	—	—	—	—	0.8	0.1	475.9
$\Sigma_c(3585)^2D_{5/2}$	80.7	46.1	126.5	10.2	23.4	200.6	1.1	68.6	4.5	9.7	0.8	23.6	7.9	2.3	14.2	0.2	96.6	0.6	—	—	—	—	—	—	2.8	1.7	722.1
$\Sigma_c(3555)^4D_{1/2}$	14.5	16.2	137.8	0.8	8.1	10.3	564.6	14.2	4.4	0.4	4.8	0.6	14.0	17.0	3.0	43.9	5.2	284.8	—	—	—	—	—	—	—	5.5	1150.1
$\Sigma_c(3582)^4D_{3/2}$	12.8	4.4	94.4	1.3	11.9	19.3	226.5	33.4	2.1	1.0	8.7	2.5	10.4	33.5	7.2	42.4	9.8	115.9	—	—	—	—	—	—	4.6	9.5	651.6
$\Sigma_c(3627)^4D_{5/2}$	12.5	68.8	64.8	1.9	17.3	13.8	21.5	62.7	6.9	2.4	9.3	4.9	15.2	20.8	5.8	17.8	6.9	10.8	—	—	—	—	—	—	32.0	16.0	412.1
$\Sigma_c(3691)^4D_{7/2}$	30.7	173.4	186.5	3.9	35.8	56.6	529.9	275.3	21.7	3.9	11.2	8.8	45.4	54.9	9.0	22.1	27.8	255.6	—	—	—	—	—	—	126.8	—	1879.3

TABLE XI. Same as IX, but for $\Xi_c'(snc)$ states. The order of the states is the same as in Table VI. The predicted masses, reported in Table VI, are obtained by the three-quark model Hamiltonian of Eqs. (1) and (2).

$\Xi_c'(snc)$ $\mathcal{F} = \mathbf{6}_{\rm f}$	$\Lambda_c K$	$\Xi_c \pi$	$\Xi_c' \pi$	$\Xi_c^* \pi$	$\Sigma_c K$	$\Sigma_c^* K$	$\Xi_c \eta$	$\Lambda_c K^*$	$\Xi_c \rho$	$\Xi_c' \rho$	$\Xi_c^* \rho$	$\Sigma_c K^*$	$\Sigma_c^* K^*$	$\Xi_c' \eta$	$\Xi_c^* \eta$	$\Xi_c \eta'$	$\Xi_c' \eta'$	$\Xi_c^* \eta'$	$\Xi_c \omega$	$\Xi_c' \omega$	$\Xi_c^* \omega$	$\Xi_c \phi$	$\Xi_c' \phi$	$\Xi_c^* \phi$	$\Sigma_8 D$	$\Xi_8 D_s$	$\Sigma_8 D^*$	$\Sigma_{10} D$	Predicted $\Gamma_{\rm tot}$
$\Xi_c'(2571)^2S_{1/2}$	0	0	0	0	0	0	0	0	0	0	0	0	0	0	0	0	0	0	0	0	0	0	0	0	0	0	0	0	0
$\Xi_c'(2640)^4S_{3/2}$	0	0.4	0	0	0	0	0	0	0	0	0	0	0	0	0	0	0	0	0	0	0	0	0	0	0	0	0	0	0.4
$\Xi_c'(2893)^2P_{1/2}$	0.7	0.4	1.1	5.1	0	0	0	0	0	0	0	0	0	0	0	0	0	0	0	0	0	0	0	0	0	0	0	0	7.3
$\Xi_c'(2935)^4P_{1/2}$	0.8	0.4	0.5	3.2	0.2	0	0	0	0	0	0	0	0	0	0	0	0	0	0	0	0	0	0	0	0	0	0	0	5.1
$\Xi_c'(2920)^2P_{3/2}$	8.3	9.5	9.4	0.7	0	0	0	0	0	0	0	0	0	0	0	0	0	0	0	0	0	0	0	0	0	0	0	0	27.9
$\Xi_c'(2962)^4P_{3/2}$	1.8	2.1	0.5	13.9	0.6	0	0	0	0	0	0	0	0	0	0	0	0	0	0	0	0	0	0	0	0	0	0	0	18.9
$\Xi_c'(3007)^4P_{5/2}$	11.3	13.4	3.6	6.2	7.4	1.1	0.1	0	0	0	0	0	0	0	0	0	0	0	0	0	0	0	0	0	—	0	0	0	43.1
$\Xi_c'(3040)^2P_{1/2}$	—	—	0.4	52.2	5.5	98.5	—	0	0	0	0	0	0	0	0	0	0	0	0	0	0	0	0	0	—	0	0	0	156.6
$\Xi_c'(3067)^2P_{3/2}$	—	—	21.7	11.9	50.4	15.9	—	0	0	0	0	0	0	0	0	0	0	0	0	0	0	0	0	0	—	0	0	0	99.9
$\Xi_c'(3223)^2D_{3/2}$	0.6	0.7	0.7	1.1	1.6	2.2	0.1	0.4	0	0	0	0	0	—	—	0	0	0	0	0	0	0	0	0	2.3	0	10.7	0.1	20.5
$\Xi_c'(3268)^2D_{5/2}$	1.8	2.2	2.2	0.3	4.6	0.6	0.2	0.1	—	0	0	0	0	0.1	—	0	0	0	—	0	0	0	0	0	6.6	0	38.0	7.8	64.5
$\Xi_c'(3238)^4D_{1/2}$	—	—	—	1.6	0.1	3.3	—	0.6	0.1	0	0	0	0	—	—	0	0	0	0	0	0	0	0	0	2.6	0	19.7	0.9	28.9
$\Xi_c'(3265)^4D_{3/2}$	0.7	0.8	0.2	2.1	0.5	4.6	0.1	1.8	0.4	0	0	0	0	—	0.1	0	0	0	0.1	0	0	0	0	0	10.2	0	27.1	4.3	53.0
$\Xi_c'(3310)^4D_{5/2}$	1.6	2.0	0.5	1.9	1.1	4.3	0.2	1.7	1.1	0	0	0	0	—	0.1	0	0	0	0.3	0	0	0	0	0	24.2	0.8	32.8	24.6	97.2
$\Xi_c'(3373)^4D_{7/2}$	2.5	3.1	0.8	2.7	1.7	5.2	0.3	2.0	1.3	—	0	0.1	0	0.1	0.1	0	0	0	0.4	—	0	0	0	0	37.4	6.9	32.7	63.2	160.5
$\Xi_c'(3250)^2S_{1/2}$	—	0.1	0.1	—	0.2	0.1	—	0.1	—	0	0	0	0	—	—	0	0	0	0	0	0	0	0	0	0.2	0	1.5	0.1	2.4
$\Xi_c'(3319)^4S_{3/2}$	—	—	—	0.1	0.1	0.3	—	0.1	0.1	0	0	0	0	—	—	0	0	0	—	0	0	0	0	0	0.5	0.1	1.3	1.8	4.4
$\Xi_c'(3544)^2S_{1/2}$	—	—	0.1	0.1	0.2	0.2	—	0.4	0.8	5.0	0.1	10.9	0.1	—	—	0.4	—	0	0.3	1.7	—	0.3	0	0	—	—	—	—	20.6
$\Xi_c'(3613)^4S_{3/2}$	0.1	—	—	0.1	—	0.2	—	0.2	0.6	0.3	7.3	0.6	15.9	—	0.1	0.4	0.1	0.1	0.2	0.1	2.4	0.6	—	0	—	—	—	—	29.3
$\Xi_c'(3370)^2D_{3/2}$	—	—	1.7	40.4	4.0	90.1	—	39.1	34.0	1.2	0	4.0	0	0.3	2.8	0	0	0	10.7	0.3	0	0	0	0	—	—	—	—	228.6
$\Xi_c'(3415)^2D_{5/2}$	—	—	22.7	11.8	48.4	22.3	—	11.3	9.1	0.8	0	2.1	0.2	1.7	0.3	0	0	0	2.9	0.2	0	0	0	0	—	—	—	—	133.8
$\Xi_c'(3379)^2P_{1/2}$	—	—	—	0.6	—	1.2	—	0.3	0.2	—	0	—	0	—	—	0	0	0	0.1	—	0	0	0	0	—	—	—	—	2.4
$\Xi_c'(3406)^2P_{3/2}$	—	—	0.4	0.3	0.8	0.7	—	0.4	0.3	—	0	—	0	—	—	0	0	0	0.1	—	0	0	0	0	—	—	—	—	3.0
$\Xi_c'(3397)^2S_{1/2}$	—	—	0.3	2.5	1.4	8.4	—	9.7	15.1	3.1	0	8.6	0	0.5	1.0	0	0	0	5.0	0.8	0	0	0	0	—	—	—	—	56.4
$\Xi_c'(3517)^2D_{3/2}$	8.4	9.4	8.1	4.5	17.2	10.6	0.6	4.2	8.9	66.7	—	151.6	0.1	0.6	0.8	1.8	0	0	3.0	21.8	—	1.4	0	0	—	—	—	—	319.7
$\Xi_c'(3563)^2D_{5/2}$	16.8	20.4	21.0	8.8	45.3	18.7	1.7	6.2	3.4	20.1	0.4	51.4	1.0	1.8	0.4	5.7	1.2	0	1.1	6.4	0.1	0.3	0	0	—	—	—	—	232.2
$\Xi_c'(3532)^4D_{1/2}$	10.4	9.7	1.2	10.0	2.3	22.6	0.2	8.5	13.8	3.9	139.6	8.8	345.6	—	1.3	1.4	0.1	0	4.6	1.3	43.9	2.6	0	0	—	—	—	—	631.8
$\Xi_c'(3559)^4D_{3/2}$	10.1	11.3	2.5	5.4	5.2	12.6	0.7	16.0	26.3	8.0	85.1	17.8	200.3	0.2	1.2	2.5	0.1	0	8.8	2.6	27.4	8.1	0	0	—	—	—	—	452.2
$\Xi_c'(3604)^4D_{5/2}$	10.9	14.3	4.1	13.5	9.0	29.3	1.4	11.9	16.2	5.2	16.9	11.2	34.4	0.4	1.2	5.8	0.6	0.4	5.4	1.7	5.7	8.2	0.2	0	—	—	—	—	207.9
$\Xi_c'(3668)^4D_{7/2}$	25.7	31.2	7.9	43.1	17.1	93.8	2.6	51.1	51.9	9.9	40.0	24.5	117.6	0.6	2.9	10.5	2.1	1.5	16.9	3.2	12.4	10.7	0.8	0.2	—	—	—	—	578.2

TABLE XII. Same as IX, but for $\Xi_c(snc)$ states. The order of the states is the same as in Table VII. The predicted masses, reported in Table VII, are obtained by the three-quark model Hamiltonian of Eqs. (1) and (2).

$\Xi_c(snc)$ $\mathcal{F}=\bar{\mathbf{3}}_{\rm f}$	$\Lambda_c K$	$\Xi_c\pi$	$\Xi'_c\pi$	$\Xi^*_c\pi$	$\Sigma_c K$	$\Sigma^*_c K$	$\Xi_c\eta$	$\Lambda_c K^*$	$\Xi_c\rho$	$\Xi'_c\rho$	$\Xi^*_c\rho$	$\Sigma_c K^*$	$\Sigma^*_c K^*$	$\Xi'_c\eta$	$\Xi^*_c\eta$	$\Xi_c\eta'$	$\Xi'_c\eta'$	$\Xi^*_c\eta'$	$\Xi_c\omega$	$\Xi'_c\omega$	$\Xi^*_c\omega$	$\Xi_c\phi$	$\Xi'_c\phi$	$\Xi^*_c\phi$	$\Lambda_8 D$	$\Lambda_8 D^*$	$\Sigma_8 D$	$\Lambda^*_8 D$	Predicted $\Gamma_{\rm tot}$
$\Xi_c(2466)^2S_{1/2}$	0	0	0	0	0	0	0	0	0	0	0	0	0	0	0	0	0	0	0	0	0	0	0	0	0	0	0	0	0
$\Xi_c(2788)^2P_{1/2}$	—	—	0.6	2.0	0	0	0	0	0	0	0	0	0	0	0	0	0	0	0	0	0	0	0	0	0	0	0	0	2.6
$\Xi_c(2815)^2P_{3/2}$	—	—	3.9	0.6	0	0	0	0	0	0	0	0	0	0	0	0	0	0	0	0	0	0	0	0	0	0	0	0	4.5
$\Xi_c(2935)^2P_{1/2}$	0.8	0.4	2.0	13.3	0.5	0	0	0	0	0	0	0	0	0	0	0	0	0	0	0	0	0	0	0	0	0	0	0	17.0
$\Xi_c(2977)^4P_{1/2}$	0.6	0.2	0.7	7.7	3.4	0.3	0	0	0	0	0	0	0	0	0	0	0	0	0	0	0	0	0	0	0	0	0	0	12.9
$\Xi_c(2962)^2P_{3/2}$	18.7	21.8	22.7	2.0	23.9	0	0	0	0	0	0	0	0	0	0	0	0	0	0	0	0	0	0	0	0	0	0	0	89.1
$\Xi_c(3004)^4P_{3/2}$	4.0	4.7	1.3	31.5	2.5	12.2	0	0	0	0	0	0	0	0	0	0	0	0	0	0	0	0	0	0	—	0	—	0	56.2
$\Xi_c(3049)^4P_{5/2}$	25.5	30.8	8.4	17.0	19.2	19.0	2.2	0	0	0	0	0	0	0	0	0	0	0	0	0	0	0	0	0	—	0	—	0	122.1
$\Xi_c(3118)^2D_{3/2}$	—	—	0.4	2.2	0.8	2.9	—	0	0	0	0	0	0	0	0	0	0	0	0	0	0	0	0	0	4.5	0.5	39.2	0	50.5
$\Xi_c(3164)^2D_{5/2}$	—	—	1.2	0.5	2.2	0.6	—	0	0	0	0	0	0	—	0	0	0	0	0	0	0	0	0	0	12.7	2.1	112.5	0	131.8
$\Xi_c(3145)^2S_{1/2}$	—	—	0.1	0.1	0.1	0.2	—	0	0	0	0	0	0	—	0	0	0	0	0	0	0	0	0	0	0.5	0.2	4.0	0	5.2
$\Xi_c(3440)^2S_{1/2}$	—	—	0.2	0.5	0.4	1.2	—	0.9	1.3	0.5	—	1.1	0.1	—	0.1	—	0	0	0.4	0.1	—	0	0	0	—	—	—	—	6.8
$\Xi_c(3265)^2D_{3/2}$	1.3	1.7	2.5	10.6	6.3	21.8	0.3	6.9	1.6	0	0	0	0	0.2	0.3	0	0	0	0.4	0	0	0	0	0	—	—	—	0	53.9
$\Xi_c(3311)^2D_{5/2}$	18.3	22.3	22.1	1.8	46.0	3.1	1.6	1.1	0.8	0	0	0	0	1.2	—	0	0	0	0.3	0	0	0	0	0	—	—	—	0	118.6
$\Xi_c(3280)^4D_{1/2}$	0.2	0.4	0.5	4.6	1.7	9.8	0.4	3.7	1.5	0	0	0	0	0.1	0.2	0	0	0	0.4	0	0	0	0	0	—	—	—	0	23.5
$\Xi_c(3307)^4D_{3/2}$	1.4	1.7	0.6	17.4	1.5	39.0	0.3	16.8	9.5	0	0	0	0	0.1	0.9	0	0	0	2.7	0	0	0	0	0	—	—	—	0	91.9
$\Xi_c(3353)^4D_{5/2}$	8.1	9.8	2.5	23.8	5.2	52.7	0.7	23.0	18.4	0.2	0	0.8	0	0.2	1.5	0	0	0	5.7	0	0	0	0	0	—	—	—	0	152.6
$\Xi_c(3416)^4D_{7/2}$	30.6	37.1	9.4	20.1	20.1	39.4	3.0	15.4	10.2	0.6	0.3	1.8	1.0	0.7	0.7	0.3	0	0	3.2	0.2	0.1	0	0	0	—	—	—	—	194.2
$\Xi_c(3274)^2P_{1/2}$	—	—	—	0.1	—	0.2	—	—	—	0	0	0	0	—	—	0	0	0	—	0	0	0	0	0	—	—	—	0	0.3
$\Xi_c(3302)^2P_{3/2}$	0.3	0.4	0.4	0.1	0.7	0.1	—	—	—	0	0	0	0	—	—	0	0	0	—	0	0	0	0	0	—	—	—	0	2.0
$\Xi_c(3316)^4P_{1/2}$	—	—	—	0.1	—	0.1	—	—	—	0	0	0	0	—	—	0	0	0	—	0	0	0	0	0	—	—	—	0	0.2
$\Xi_c(3344)^4P_{3/2}$	0.1	0.1	—	0.3	—	0.5	—	0.2	0.1	0	0	0	0	—	—	0	0	0	—	0	0	0	0	0	—	—	—	0	1.3
$\Xi_c(3389)^4P_{5/2}$	0.5	0.6	0.1	0.4	0.3	0.9	—	0.4	0.3	—	0	—	0	—	—	0	0	0	0.1	—	0	0	0	0	—	—	—	—	3.6
$\Xi_c(3362)^4S_{3/2}$	0.9	0.3	0.3	3.1	1.0	9.7	0.3	7.2	8.7	0.2	0	0.8	0	0.2	0.7	0	0	0	2.8	0.1	0	0	0	0	—	—	—	0	36.3
$\Xi_c(3293)^2S_{1/2}$	0.1	0.3	2.5	1.9	8.0	5.3	0.4	6.2	3.4	0	0	0	0	0.6	0.2	0	0	0	0.9	0	0	0	0	0	—	—	—	0	29.8
$\Xi_c(3413)^2D_{3/2}$	—	—	4.1	16.4	8.7	38.9	—	19.5	23.1	3.3	0	8.7	0	0.3	1.9	0	0	0	7.5	0.9	0	0	0	0	—	—	—	—	133.3
$\Xi_c(3458)^2D_{5/2}$	—	—	12.0	15.2	25.7	30.5	—	14.7	12.2	0.4	0.3	0.8	1.0	1.0	0.5	—	0	0	3.9	0.1	0.1	0	0	0	—	—	—	—	118.4

TABLE XIII. Same as IX, but for $\Lambda_c(nnc)$ states. The order of the states is the same as in Table VIII. The predicted masses, reported in Table VIII, are obtained by the three-quark model Hamiltonian of Eqs. (1) and (2).

$\Lambda_c(nnc)$ $\mathcal{F} = \bar{\mathbf{3}}_{\rm f}$	$\Sigma_c\pi$	$\Sigma_c^*\pi$	$\Lambda_c\eta$	$\Sigma_c\rho$	$\Sigma^*\rho$	$\Lambda_c\eta'$	$\Lambda_c\omega$	$\Xi_c K$	$\Xi_c' K$	$\Xi_c^* K$	$\Xi_c K^*$	$\Xi_c' K^*$	$\Xi_c^* K^*$	ND	Predicted $\Gamma_{\rm tot}$
$\Lambda_c(2261)^2S_{1/2}$	0	0	0	0	0	0	0	0	0	0	0	0	0	0	0
$\Lambda_c(2616)^2P_{1/2}$	1.4	0	0	0	0	0	0	0	0	0	0	0	0	0	1.4
$\Lambda_c(2643)^2P_{3/2}$	9.7	0.1	0	0	0	0	0	0	0	0	0	0	0	0	9.8
$\Lambda_c(2799)^2P_{1/2}$	7.3	49.6	0	0	0	0	0	0	0	0	0	0	0	0	56.9
$\Lambda_c(2841)^4P_{1/2}$	2.6	28.5	1.4	0	0	0	0	0	0	0	0	0	0	—	32.5
$\Lambda_c(2826)^2P_{3/2}$	83.9	7.7	1.1	0	0	0	0	0	0	0	0	0	0	—	92.7
$\Lambda_c(2868)^4P_{3/2}$	4.7	115.8	1.4	0	0	0	0	0	0	0	0	0	0	—	121.9
$\Lambda_c(2913)^4P_{5/2}$	31.2	64.6	12.2	0	0	0	0	0.1	0	0	0	0	0	—	108.1
$\Lambda_c(2980)^2D_{3/2}$	1.7	8.8	—	0	0	0	0	—	0	0	0	0	0	59.1	69.6
$\Lambda_c(3025)^2D_{5/2}$	4.7	2.0	—	0	0	0	0	—	0	0	0	0	0	164.5	171.2
$\Lambda_c(3007)^2S_{1/2}$	0.2	0.4	—	0	0	0	0	—	0	0	0	0	0	4.7	5.3
$\Lambda_c(3372)^2S_{1/2}$	0.2	0.7	—	2.5	0.4	—	1.1	—	0.4	0.8	0.2	0	0	—	6.3
$\Lambda_c(3163)^2D_{3/2}$	9.0	42.0	1.0	0	0	0	13.3	2.7	1.6	0.7	0	0	0	—	70.3
$\Lambda_c(3208)^2D_{5/2}$	90.0	10.1	8.3	0.4	0	0	1.7	13.9	8.4	0.2	0	0	0	—	133.0
$\Lambda_c(3178)^4D_{1/2}$	1.0	19.9	0.6	0	0	0	7.5	3.8	0.8	0.7	0	0	0	—	34.3
$\Lambda_c(3205)^4D_{3/2}$	2.2	63.0	0.9	0.4	0	0	31.5	2.9	0.6	4.5	0	0	0	—	106.0
$\Lambda_c(3250)^4D_{5/2}$	10.3	86.6	3.8	3.9	0.1	0.2	39.9	6.7	1.2	10.0	0	0	0	—	162.7
$\Lambda_c(3313)^4D_{7/2}$	37.3	99.2	13.9	4.5	2.8	5.7	29.8	26.8	5.7	4.4	0	0	0	—	230.1
$\Lambda_c(3172)^2P_{1/2}$	—	0.4	—	0	0	0	0.1	—	—	—	0	0	0	—	0.5
$\Lambda_c(3199)^2P_{3/2}$	1.2	0.3	0.1	0	0	0	—	0.2	0.1	—	0	0	0	—	1.9
$\Lambda_c(3214)^4P_{1/2}$	—	0.3	—	0	0	0	—	—	—	—	0	0	0	—	0.3
$\Lambda_c(3241)^4P_{3/2}$	0.1	0.9	—	—	0	0	0.3	—	—	—	0	0	0	—	1.3
$\Lambda_c(3286)^4P_{5/2}$	0.5	1.4	0.2	0.1	0	—	0.6	0.3	0.1	0.1	0	0	0	—	3.3
$\Lambda_c(3259)^4S_{3/2}$	0.3	4.7	0.2	2.9	1.2	0.7	11.2	3.9	1.6	5.6	0	0	0	—	32.3
$\Lambda_c(3190)^2S_{1/2}$	4.1	4.4	0.7	0.1	0	0	10.8	4.8	4.4	0.8	0	0	0	—	30.1
$\Lambda_c(3345)^2D_{3/2}$	21.0	49.6	—	26.4	0.3	—	33.3	—	3.5	18.8	0.7	0	0	—	153.6
$\Lambda_c(3390)^2D_{5/2}$	54.3	90.1	—	2.1	3.8	—	34.5	—	10.0	5.4	1.5	0	0	—	201.7

APPENDIX G: DECAY PRODUCTS

TABLE XIV. Masses of final state baryons and mesons used in the calculation of the decay widths as from PDG [9].

	Mass in GeV
m_π	0.13725 ± 0.00295
m_K	0.49564 ± 0.00279
m_η	0.54786 ± 0.00002
$m_{\eta'}$	0.95778 ± 0.00006
m_ρ	0.77518 ± 0.00045
m_{K^*}	0.89555 ± 0.00100
m_ω	0.78266 ± 0.00002
m_ϕ	1.01946 ± 0.00002
m_D	1.86672 ± 0.00193
m_{D_s}	1.96835 ± 0.00007
m_{D^*}	2.00855 ± 0.00180
m_N	0.93891 ± 0.00091
$m_{N(1520)}$	1.51500 ± 0.00500
$m_{N(1535)}$	1.53000 ± 0.01500
$m_{N(1680)}$	1.68500 ± 0.00500
$m_{N(1720)}$	1.72000 ± 0.03500
m_Δ	1.23200 ± 0.00200
m_Λ	1.11568 ± 0.00001
$m_{\Lambda(1520)}$	1.51900 ± 0.00010
m_{Ξ_8}	1.31820 ± 0.00360
$m_{\Xi_{10}}$	1.53370 ± 0.00250
m_{Σ_8}	1.11932 ± 0.00340
$m_{\Sigma_{10}}$	1.38460 ± 0.00460
m_{Λ_c}	2.28646 ± 0.00014
m_{Ξ_c}	2.46908 ± 0.00158
$m_{\Xi'_c}$	2.57850 ± 0.00100
$m_{\Xi^*_c}$	2.64563 ± 0.00100
m_{Σ_c}	2.45350 ± 0.00090
$m_{\Sigma^*_c}$	2.51813 ± 0.00280
m_{Ω_c}	2.69520 ± 0.00170
$m_{\Omega^*_c}$	2.76590 ± 0.00200

[1] R. Aaij *et al.*, Phys. Rev. Lett. **118**, 182001 (2017).
[2] J. Yelton *et al.* (Belle Collaboration), Phys. Rev. D **97**, 051102 (2018).
[3] R. Aaij *et al.*, Phys. Rev. Lett. **124**, 222001 (2020).
[4] Y. B. Li *et al.*, Eur. Phys. J. C **78**, 252 (2018).
[5] B. Aubert *et al.*, Phys. Rev. D **77**, 031101 (2008).
[6] J. Yelton *et al.*, Phys. Rev. D **94**, 052011 (2016).
[7] R. Chistov *et al.*, Phys. Rev. Lett. **97**, 162001 (2006).
[8] B. Aubert *et al.*, Phys. Rev. D **77**, 012002 (2008).
[9] P. Zyla *et al.*, Prog. Theor. Exp. Phys. **2020**, 083C01 (2020).
[10] J. Yelton *et al.*, Phys. Rev. D **104**, 052003 (2021).
[11] T. J. Moon *et al.* (Belle Collaboration), Phys. Rev. D **103**, L111101 (2021).
[12] N. Isgur and G. Karl, Phys. Lett. **72B**, 109 (1977).

[13] N. Isgur and G. Karl, Phys. Rev. D **18**, 4187 (1978).
[14] L. A. Copley, N. Isgur, and G. Karl, Phys. Rev. D **20**, 768 (1979); **23**, 817(E) (1981).
[15] S. Capstick and N. Isgur, AIP Conf. Proc. **132**, 267 (1985).
[16] D. Ebert, R. N. Faustov, and V. O. Galkin, Phys. Rev. D **84**, 014025 (2011).
[17] D. Ebert, R. N. Faustov, and V. O. Galkin, Phys. Lett. B **659**, 612 (2008).
[18] W. Roberts and M. Pervin, Int. J. Mod. Phys. A **23**, 2817 (2008).
[19] T. Yoshida, E. Hiyama, A. Hosaka, M. Oka, and K. Sadato, Phys. Rev. D **92**, 114029 (2015).
[20] B. Chen, K. W. Wei, X. Liu, and T. Matsuki, Eur. Phys. J. C **77**, 154 (2017).
[21] H. X. Chen, W. Chen, Q. Mao, A. Hosaka, X. Liu, and S. L. Zhu, Phys. Rev. D **91**, 054034 (2015).
[22] H. X. Chen, Q. Mao, A. Hosaka, X. Liu, and S. L. Zhu, Phys. Rev. D **94**, 114016 (2016).
[23] E. Bagan, M. Chabab, H. G. Dosch, and S. Narison, Phys. Lett. B **287**, 176 (1992).
[24] H. M. Yang and H. X. Chen, Phys. Rev. D **104**, 034037 (2021).
[25] L. X. Gutiérrez-Guerrero, A. Bashir, M. A. Bedolla, and E. Santopinto, Phys. Rev. D **100**, 114032 (2019).
[26] H. Garcilazo, J. Vijande, and A. Valcarce, J. Phys. G **34**, 961 (2007).
[27] P. Hasenfratz, R. R. Horgan, J. Kuti, and J. M. Richard, Phys. Lett. **94B**, 401 (1980).
[28] M. J. Savage, Phys. Lett. B **359**, 189 (1995).
[29] Y. Kim, E. Hiyama, M. Oka, and K. Suzuki, Phys. Rev. D **102**, 014004 (2020).
[30] Y. Kim, Y. R. Liu, M. Oka, and K. Suzuki, Phys. Rev. D **104**, 054012 (2021).
[31] J. Vijande, A. Valcarce, and H. Garcilazo, Phys. Rev. D **90**, 094004 (2014).
[32] L. Liu, H. W. Lin, K. Orginos, and A. Walker-Loud, Phys. Rev. D **81**, 094505 (2010).
[33] R. A. Briceno, H. W. Lin, and D. R. Bolton, Phys. Rev. D **86**, 094504 (2012).
[34] H. Bahtiyar, K. U. Can, G. Erkol, P. Gubler, M. Oka, and T. T. Takahashi, Phys. Rev. D **102**, 054513 (2020).
[35] J. G. Korner, M. Kramer, and D. Pirjol, Prog. Part. Nucl. Phys. **33**, 787 (1994).
[36] H. X. Chen, W. Chen, X. Liu, Y. R. Liu, and S. L. Zhu, Rep. Prog. Phys. **80**, 076201 (2017).
[37] V. Crede and W. Roberts, Rep. Prog. Phys. **76**, 076301 (2013).
[38] Y. S. Amhis *et al.*, Eur. Phys. J. C **81**, 226 (2021).
[39] H. Y. Cheng, Front. Phys. (Beijing) **10**, 101406 (2015).
[40] X. H. Zhong and Q. Zhao, Phys. Rev. D **77**, 074008 (2008).
[41] L. H. Liu, L. Y. Xiao, and X. H. Zhong, Phys. Rev. D **86**, 034024 (2012).
[42] K. L. Wang, Y. X. Yao, and X. H. Zhong, Q. Zhao, Phys. Rev. D **96**, 116016 (2017).
[43] K. L. Wang, L. Y. Xiao, X. H. Zhong, and Q. Zhao, Phys. Rev. D **95**, 116010 (2017).
[44] H. Y. Cheng and C. K. Chua, Phys. Rev. D **75**, 014006 (2007).
[45] H. Y. Cheng and C. K. Chua, Phys. Rev. D **92**, 074014 (2015).
[46] H. Nagahiro, S. Yasui, A. Hosaka, M. Oka, and H. Noumi, Phys. Rev. D **95**, 014023 (2017).
[47] A. J. Arifi, D. Suenaga, and A. Hosaka, Phys. Rev. D **103**, 094003 (2021).
[48] Y. X. Yao, K. L. Wang, and X. H. Zhong, Phys. Rev. D **98**, 076015 (2018).
[49] S. L. Zhu, Phys. Rev. D **61**, 114019 (2000).
[50] H. X. Chen, Q. Mao, W. Chen, A. Hosaka, X. Liu, and S. L. Zhu, Phys. Rev. D **95**, 094008 (2017).
[51] C. Chen, X. L. Chen, X. Liu, W. Z. Deng, and S. L. Zhu, Phys. Rev. D **75**, 094017 (2007).
[52] J. J. Guo, P. Yang, and A. Zhang, Phys. Rev. D **100**, 014001 (2019).
[53] K. Gong, H. Y. Jing, and A. Zhang, Eur. Phys. J. C **81**, 467 (2021).
[54] Q. F. Lü, L. Y. Xiao, Z. Y. Wang, and X. H. Zhong, Eur. Phys. J. C **78**, 599 (2018).
[55] E. Santopinto, A. Giachino, J. Ferretti, H. García-Tecocoatzi, M. A. Bedolla, R. Bijker, and E. Ortiz-Pacheco, Eur. Phys. J. C **79**, 1012 (2019).
[56] R. Bijker, H. García-Tecocoatzi, A. Giachino, E. Ortiz-Pacheco, and E. Santopinto, Phys. Rev. D **105**, 074029 (2022).
[57] B. Efron and R. J. Tibshirani, *An Introduction to the Bootstrap*, Monographs on Statistics and Applied Probability (Chapman and Hall, London, 1993).
[58] S. Capstick and W. Roberts, Phys. Rev. D **47**, 1994 (1993).
[59] N. Isgur and G. Karl, Phys. Rev. D **18**, 4187 (1978).
[60] L. Micu, Nucl. Phys. **B10**, 521 (1969).
[61] A. Le Yaouanc, L. Oliver, O. Pène, and J. C. Raynal, Phys. Rev. D **8**, 2223 (1973).
[62] R. Bijker, J. Ferretti, G. Galatà, H. García-Tecocoatzi, and E. Santopinto, Phys. Rev. D **94**, 074040 (2016).
[63] S. Godfrey and N. Isgur, Phys. Rev. D **32**, 189 (1985).
[64] R. Kokoski and N. Isgur, Phys. Rev. D **35**, 907 (1987).
[65] F. E. Close and E. S. Swanson, Phys. Rev. D **72**, 094004 (2005).
[66] H. G. Blundell and S. Godfrey, Phys. Rev. D **53**, 3700 (1996).
[67] D. Molina, M. De Sanctis, C. Fernández-Ramírez, and E. Santopinto, Eur. Phys. J. C **80**, 526 (2020).
[68] F. James and M. Roos, Comput. Phys. Commun. **10**, 343 (1975).
[69] C. R. Harris *et al.*, Nature (London) **585**, 357 (2020).
[70] M. Tanabashi, Phys. Rev. D **98**, 030001 (2018).
[71] M. Padmanath and N. Mathur, Phys. Rev. Lett. **119**, 042001 (2017).
[72] M. Karliner and J. L. Rosner, Phys. Rev. D **95**, 114012 (2017).
[73] Z. G. Wang, Eur. Phys. J. C **77**, 325 (2017).
[74] R. Aaij *et al.* (LHCb Collaboration), Phys. Rev. D **104**, L091102 (2021).
[75] K. L. Wang and X. H. Zhong, Chin. Phys. C **46**, 023103 (2022).
[76] H. M. Yang, H. X. Chen, and Q. Mao, Phys. Rev. D **102**, 114009 (2020).
[77] K. L. Wang, L. Y. Xiao, and X. H. Zhong, Phys. Rev. D **102**, 034029 (2020).
[78] B. Chen, X. Liu, and A. Zhang, Phys. Rev. D **95**, 074022 (2017).
[79] J. J. de Swart, Rev. Mod. Phys. **35**, 916 (1963); **37**, 326(E) (1965).